ENVIRONMENTAL RESEARCH
INFRASTRUCTURE AND SUSTAINABILITY

PURPOSE-LED PUBLISHING™

Part of the ENVIRONMENTAL RESEARCH SERIES

PAPER • OPEN ACCESS

Agent-based socio-spatial modelling of coupled human-flood interactions along the UK coast

To cite this article: Morgan J Breen *et al* 2025 *Environ. Res.: Infrastruct. Sustain.* **5** 025013

IOP Publishing Environ. Res.: Infrastruct. Sustain. 5 (2025) 025013 https://doi.org/10.1088/2634-4505/addeeb

ENVIRONMENTAL RESEARCH
INFRASTRUCTURE AND SUSTAINABILITY

OPEN ACCESS

RECEIVED
26 February 2025

REVISED
25 April 2025

ACCEPTED FOR PUBLICATION
30 May 2025

PUBLISHED
10 June 2025

PAPER

Agent-based socio-spatial modelling of coupled human-flood interactions along the UK coast

Morgan J Breen[1,*], **Abiy S Kebede**[1] and **Carola S König**[2]

[1] Department of Civil and Environmental Engineering, Brunel University London, UB8 3PH Uxbridge, United Kingdom
[2] Department of Mechanical and Aerospace Engineering, Brunel University London, UB8 3PH Uxbridge, United Kingdom
[*] Author to whom any correspondence should be addressed.

E-mail: morgan.breen@brunel.ac.uk

Keywords: agent-based modelling (ABM), socio-hydrological systems, safe development paradox, human-flood interactions, flood risk management, climate change adaptation

Abstract

This study uses agent-based modelling (ABM) to assess the socio-hydrological impacts of structural coastal flood protections (SCFPs) under different climate change scenarios considering three contrasting UK case studies: Southport, Weston-super-Mare (WSM), and Portsmouth. By integrating extreme coastal water level (ECWL) projections and population dynamics, the ABM simulations reveal five distinct phases: *Design, Implementation, Latency, Flood*, and *Post-Flood*. The results highlight that the Latency phase, whereby SCFP initially stabilises affected population (AfP), inadvertently encourages population growth in residual risk areas. This process exacerbates long-term flood exposure, leading to significant increases in AfP when ECWL exceeds the SCFP crest height, negating gains in flood protection from the initial construction/upgrade. As such, Southport and WSM saw a significant increase in coastal population within protected floodplains, with these populations potentially having limited experience with flooding, preparedness, and consequently heightened vulnerability. Conversely, Portsmouth, with limited residential development near SCFPs, demonstrated how existing land-use and high population density can reduce the unintended socio-hydrological consequences of SCFPs in densely-populated coastal settings. These findings reveal two key pathways that influence coastal population in response to SCFPs: *Land-use Driven*, where non-residential land-use limits population increase, and *Population Driven*, where high-density areas limit further growth. This study advances our understanding of the coupled human-flood dynamics by evaluating how SCFPs can increase flood impacts in the long-term by influencing socio-spatial distribution over the short- to medium-term. Moreover, it demonstrates how ABMs can provide valuable insights by simulating complex coupled human-flood dynamics; critical for supporting adaptive, resilient coastal management strategies in a changing climate.

1. Introduction

Natural hazards, such as flooding, often lead to significant socio-economic losses and environmental impacts worldwide (Sharples *et al* 2016, Natho and Thieken 2018). The impacts of climate change and continued urban development in flood-prone areas exacerbate these risks (Gbadegesin *et al* 2011, Leichenko 2011). It is therefore critical to manage these risks, both current and future, to protect our communities and infrastructure. In many instances, structural measures are often selected as the hazard mitigation strategy, such as, flood control channels (as in Sanders and Grant 2020), levees (as in Vora *et al* 2018), and seawalls (as in Betzold and Mohamed 2016). However, numerous scholars, starting with White (1945), have shown that increasing levels of structural flood protection can result in unintended consequences (Tobin 1995, Burby 2006, Kates *et al* 2006, Burton and Cutter 2008, Montz and Tobin 2008, Ludy and Kondolf 2012, Di Baldassarre *et al* 2013a). If the growth of coastal urban areas were driven by population increases alone, the spatial distribution of new settlements would be the same (Di Baldassarre *et al* 2013b). The cycle continues as

greater populations and high-value assets are placed either within or in close proximity of floodable areas, producing a need for even greater structural strengthening and/or heightening (or expansion) of existing structures. Increased safety can induce increased urban development, for example, ultimately leading to high losses in the event of a structural failure (Kates *et al* 2006). This coupled human-flood phenomena has been referred to as the Safe Development Paradox (SDP) (Burby 2006), *Levee Effect* (Di Baldassarre *et al* 2015), and *Safety Dilemma* (Di Baldassarre *et al* 2018).

Moreover, recent studies have demonstrated that expansion into high-risk flood areas have accelerated significantly since 2000, particularly in the most hazard-prone areas (Tellman *et al* 2021). Additionally, satellite data has also shown a 20%–24% rise in global flood exposure between 2000 and 2015, far exceeding previous estimates (Andreadis *et al* 2022). These findings underscore the importance of spatially explicit modelling approaches, such as agent-based models (ABMs), in the comprehension of evolving socio-hydrological processes and the unintended consequences of structural flood protection in urban areas.

Understanding the coupled human-flood dynamics of these unintended consequences of structural coastal flood protection (SCFP) and comprehending them as a function of coastal flood risk and poor spatial planning is essential in the wake of climate change and induced sea-level rise (SLR) and increased storminess. Research of these unintended consequences in fluvial environments is increasing, but there remains a notable gap in the literature regarding the specific challenges and interactions that arise in coastal environments, and the socio-hydrological and socio-spatial interactions thereof (Breen *et al* 2022). Almost 70% of literature regarding this topic was focused on flooding from rivers, compared to 17% in just coastal (Breen *et al* 2022), meanwhile, between 1970 and 2010, floodable coastal areas globally have seen 13.3% increase in population, whereas fluvial floodable areas saw a 0.5% decrease (Jongman *et al* 2012). Moreover, urban encroachment into high flood probability areas has intensified since 1985 in many areas of Asia, Europe, and North America, and since the year 2000, the rate of urban expansion into floodplains has increased by a factor of 1.5 (Andreadis *et al* 2022). This knowledge gap presents a challenge, particularly for coastal urban areas, where socio-spatial and socio-economic factors and existing land-use patterns may intensify the unintended socio-hydrological impacts of SCFPs, understanding these phenomena are essential (Loucks 2015).

This paper expands upon prior research into the unintended consequences of SCFPs by developing an ABM, a computational modelling method that simulates interactions between individual agents and their environment to understand complex systems (An 2012). Allowing for the incorporation of heterogeneous behaviours, spatial dynamics, and adaptive responses of communities to coastal flooding (Haer *et al* 2020). Within this study, ABM was used to simulate how these coupled human-flood processes and dynamics evolve across three contrasting UK case studies (figure 1): Southport, Weston-super-Mare (WSM), and Portsmouth. Each site faces unique challenges: the low-lying areas and saltmarshes of Southport will see increasing coastal flood frequency due to rising sea levels and storm surges (SSs); WSM is vulnerable to tidal (T) flooding, exacerbated by its position on the Bristol Channel, where some of the highest T ranges in the world; and Portsmouth, a densely populated coastal city which is at significant risk of flooding from both extreme T events and SSs. By simulating the potential future impacts of extreme coastal water levels (ECWLs) under various future climate scenarios, this study seeks to understand how SCFPs influence population growth and socio-spatial changes in protected areas, and to quantify the subsequent impacts when the ECWL exceeds the crest height of the SCFP, flooding areas initially protected.

The ABM simulation incorporated real-world elevation, sea level, and population spatial data, as well as projections for SLR, and changes in population distribution and socio-spatial processes associated with the construction, or major upgrade, of the local SCFP. The study showed an increase in SCFP-adjacent affected population (AfP) following construction/upgrade, a conclusion supported by current literature (e.g. Di Baldassarre *et al* 2018, Haer *et al* 2020). This demonstrates that there are lock-in processes in coastal areas in the UK. This paper concludes by discussing the limitations of ABMs in representing real-world flood dynamics, while also emphasising their unique ability to integrate geographical, sociological, and environmental factors. By advancing our understanding of the emergent socio-hydrological consequences of coastal flood protection, this study aims to inform adaptive management strategies that balance urban development and flood resilience.

2. Data & methods

2.1. Hydrometry and SLR

SLR, SS, T and wave height (WH) data were used for modelling ECWL used as input to the ABMs. These were provided by the UK Met Office and Environment Agency and were the most recent and highest quality data available.

$$\mathrm{ECWL} = \mathrm{SLR} + \mathrm{SS} + \mathrm{T} + \mathrm{WH}. \quad (1)$$

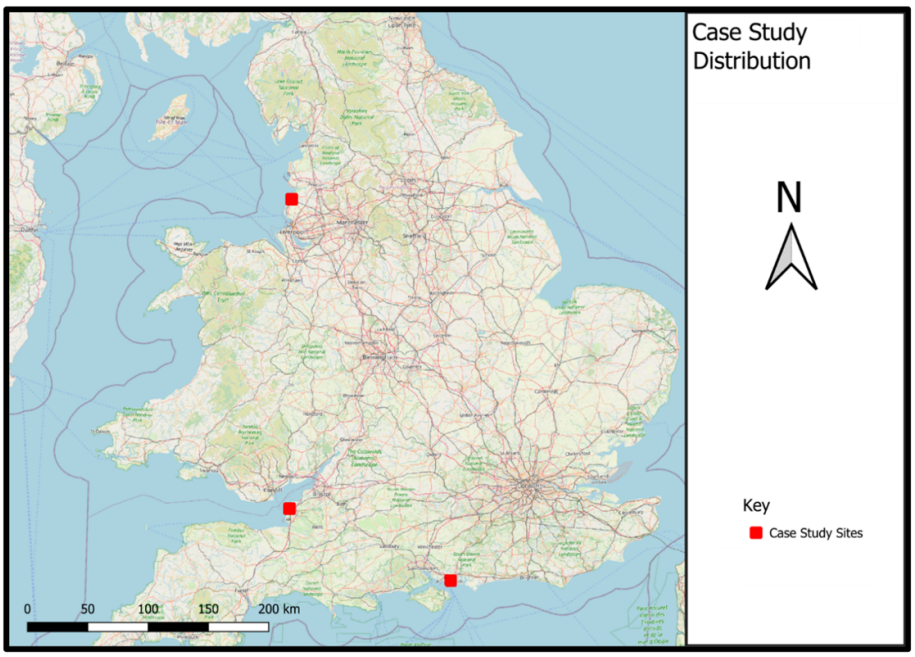

Figure 1. The distribution of case studies across the UK.

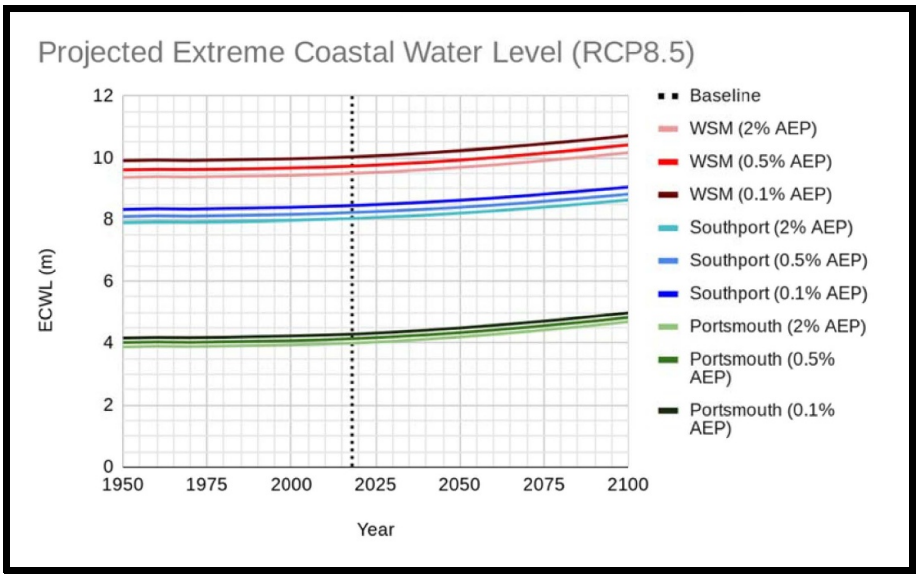

Figure 2. Historic and projected (1950–2100) ECWLs at the case studies under the RCP8.5 scenario.

The following graphs present ECWL up to 2100 under the RCP8.5 scenario, derived using equation (1), for each case study: Southport, shown in blue; WSM, shown in red; and Portsmouth, shown in green (figure 2). The lighter shades represent a 2%AEP (Annul Exceedance Probability) flood event (i.e. a 2% chance of occurring each year), the core colour represents a 0.5%AEP flood event, and finally the darkest shades represent a 0.1%AEP event, the most extreme considered within this analysis.

2.2. ABM

The use of ABMs in flood risk analysis and management is growing: Sobiech (2013) developed an ABM of coastal flooding in Germany with the aim of simulating the dynamics of vulnerability, focusing on the social context and preconceptions in which decisions, when a flood event occurs, are taken. Whereas McNamara and Keeler (2013) link sociological and physical models in their ABM, simulating the impact on the housing market of sea-level rise and increase in storminess on the American East Coast. Similarly, Chandra-Putra *et al* (2015) developed an ABM to simulate the effect of sea-level rise and insurance programmes on where

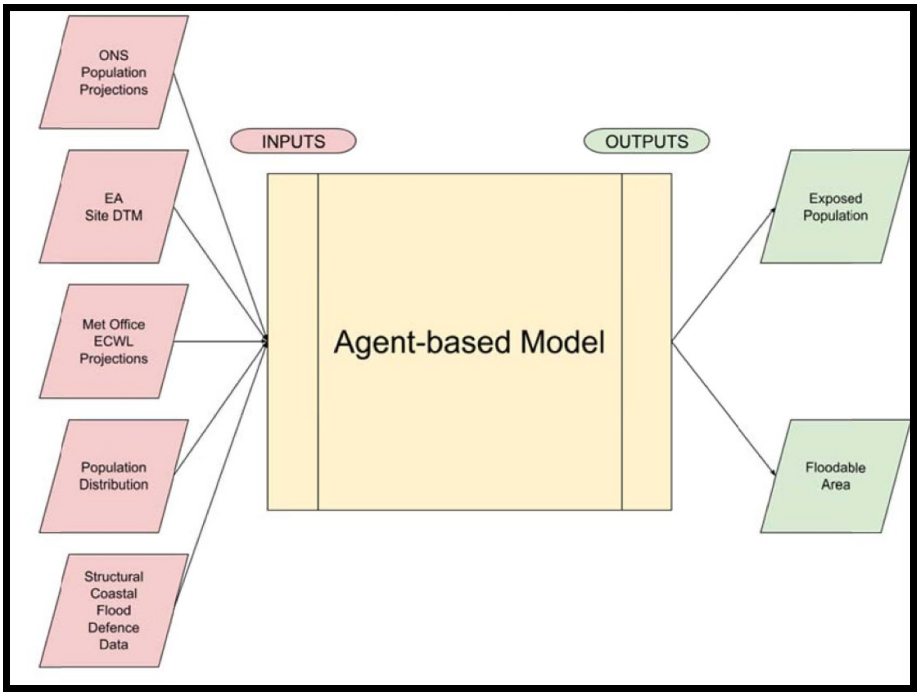

Figure 3. ABM inputs (red) and outputs (green).

people choose to live. Du *et al* (2017) developed an ABM to understand the coupling between public opinion and flood evacuation processes, and how these dynamics are influenced.

The ABM interface used for this study was the NetLogo platform and language (as in Dawson *et al* 2011), and had five inputs (figure 3): population data, both, historic and projections (from the Office for National Statistics, ONS); the LiDAR composite digital terrain model (DTM) data (from the Environment Agency, EA); ECWLs, historic and projections (from the Met Office); population distribution vectors; and SCFP projects, construction date and height obtained from government/council documentation. These inputs are processed by the ABM to produce two key outputs: (1) the size of population living in floodable areas AfP, and (2) the floodable area (FA) (FA: the ratio of dry land to flooded land at each iteration).

The backdrop of the ABM is a DTM of the location, with a resolution of 100 m $\times$ 100 m. Cells were assigned three-dimensional values, x as longitude, y as latitude, and z as elevation. To increase processing speed, polynomial equations were used to model population, developed using ONS' projections. Treating population count as the y-axis, time as the x-axis, and historic population and population projections as points, an equation was derived. This equation was verified using R-squared: if the polynomial estimated the data with a high enough R-squared ($R^2 \geqslant 0.99$, when $1991 \leqslant x \leqslant 2043$), then it could be used to represent the data. An R-Squared of 0.99 was selected as satisfactory as it was an approximation of the acceptable ONS error of 0.96%. Beyond 2043, towards 2100, the accuracy of the ABM decreases, as the ABM runs on the polynomial and without ONS projections. Past 2043, the polynomial follows the trend from the last vertex within the ONS population data, and carries that trend onto 2100 to explore long-term implications of population changes. The output of this equation each year forms the *Total Population.*

A secondary parameter that is key to the ABM is *Population Share*, the share of the settlement-wide population that an individual cell has. The product of the *Total Population* and the *Population Share* of the cells produces the *Population Distribution* for that year. However, after 2021 there is no population spatial distribution data or high-resolution population data as the censuses have not been taken yet. To resolve this, a *Population Share Change Rate* was calculated. This was determined by spatially linking and numerically comparing the 2011 and 2021 *Population Share* vectors (figure 4(a)) and obtaining a rate that reflects the change over time. The *Population Share Rate Change* vectors were supported by the geostatistical testing conducted on the boundaries with real-world Population and comparing the difference across time between those census Output Areas (OAs, which represent the lowest level of geographical area for census statistics) at the coastline and those elsewhere in the town. A statistically significant difference would give strength to the *Population Share Rate Change* as it would suggest that the patterns and trends observed from the rate change at the coastline compared to those landward of the defence are valuable and should be continued (as in Schoppa *et al* 2024).

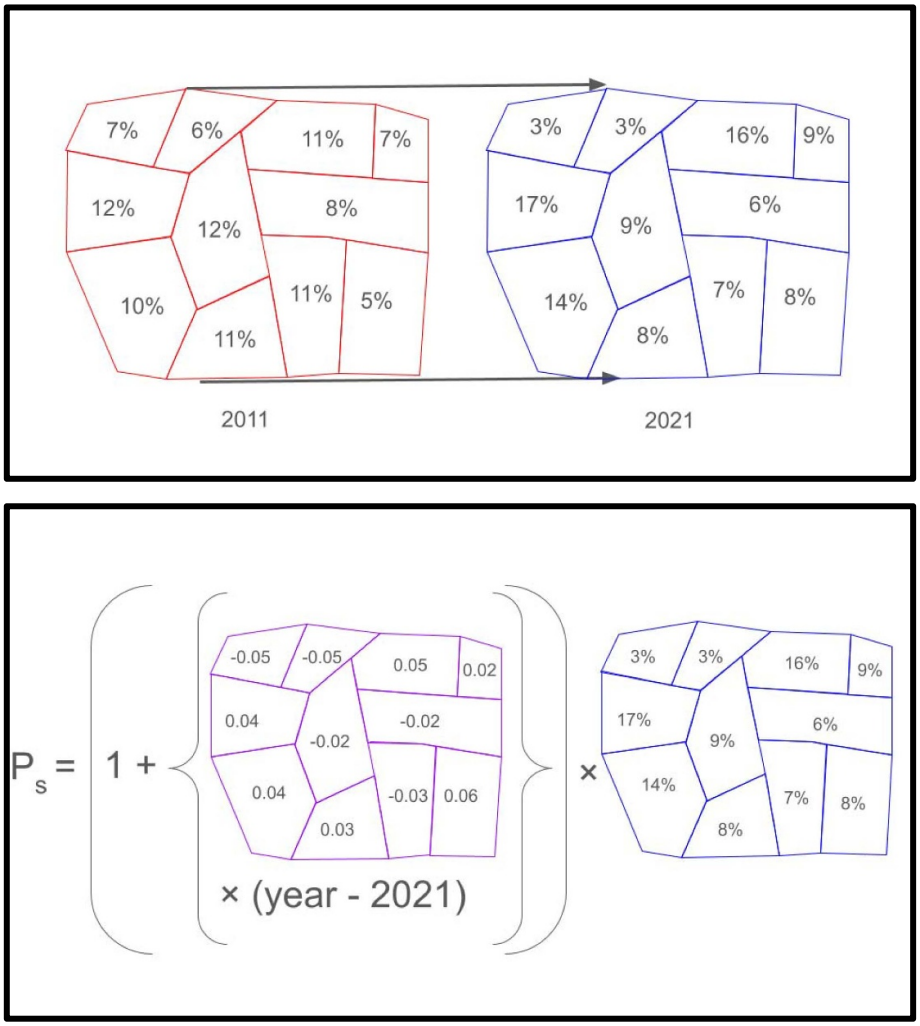

Figure 4. (a) *Population share* of a hypothetical settlement and the comparison of it across time, from the 2011 (in red) census compared to the 2021 (in blue) census; (b) modelled equation to produce *population share* (P_S) beyond 2021, the *population share rate change* vector (in purple) and the 2021 *population share* (in blue).

Then, to calculate the *Population Share* following the 2021 census, the *Population Share Rate Change* is multiplied by the current year of the ABM subtracted by 2021, to obtain years elapsed. These changes are then also multiplied by the 2021 *Population Share* vector to yield how the *Population Share Rate Change* has changed over time, and thus the *Population Share* for that year (figure 4(b)). Consequently, the product of the *Population Share* and *Total Population* of a given year post-2021 gives the modelled *Population Distribution*. This *Population Distribution* is then applied to the ABM and the flood model is run.

Once a cell comes into contact with the floodwater it is marked as *flooded*, and the AfP is summated. At the end of each year the land area is reset and the *flooded* cells returned to their normal state for the next iteration. Each year the sea rises following the ECWL scenarios. In a similar manner to population approximation, annual ECWL changes were interpolated using a polynomial and the Met Office decadal predictions as datapoints, ensuring that ECWL was continuous. The SCFP is represented using real-world dimensions and location in the ABM. Once the ECWL is higher than the SCFP the land around it is assumed that areas are flooded, this happens cell by cell until the floodwater cannot go any further due to the elevation of the land surrounding it (as in figure 5). This is one of the key strengths of ABM, allowing the integration of spatial and temporal dynamics, and modelling long-term responses to environmental change (Haer *et al* 2016, Han *et al* 2020). Although, in this ABM, future SCFP development was not considered due to the complexity of projecting policy, and heights and locations of future strengthening. However, whilst out of the scope of this paper, it is the hope that this paper will provide a springboard for such research.

2.2.1. Model set-up and runs

The agent-based socio-hydrological model (ABM) has five main stages (figure 6): Set-up, Populate, FRM (Flood Risk Management), Flood, and Export.

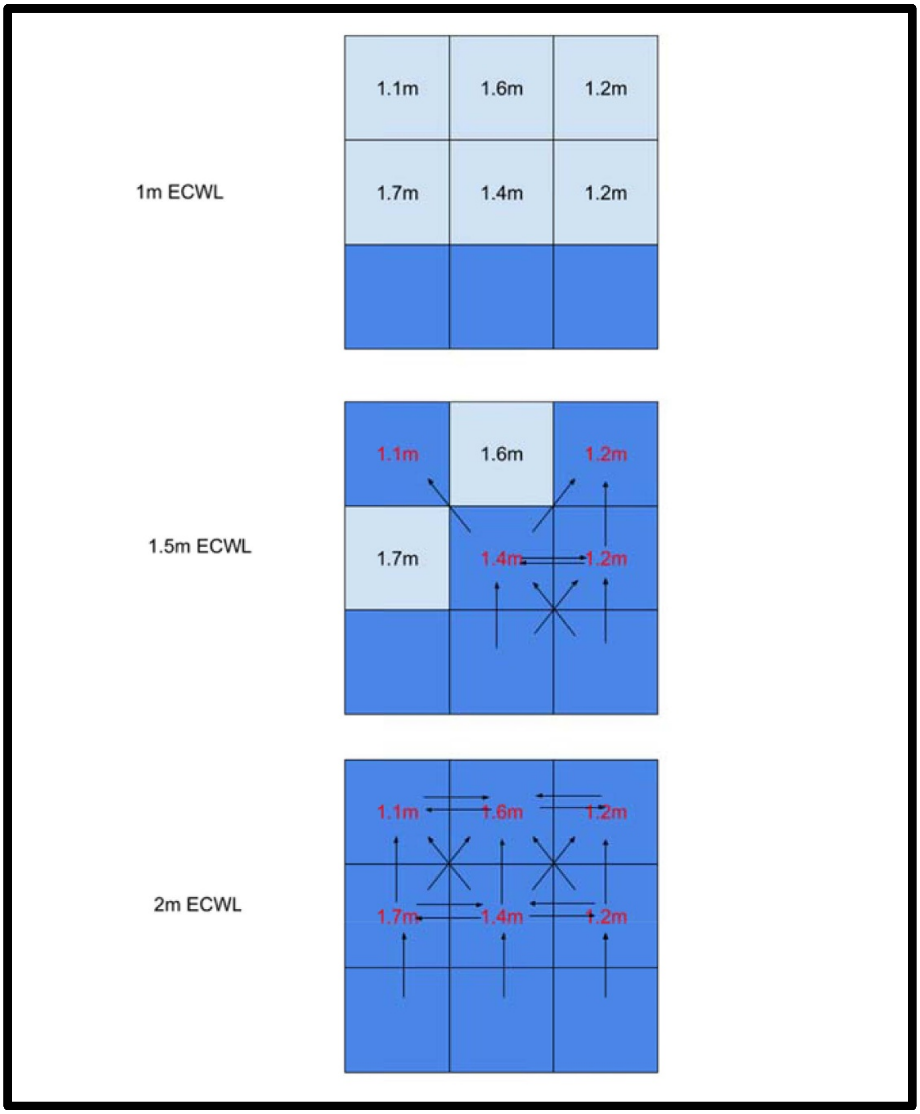

Figure 5. Illustration of the processes by which cells become flooded by the sea, if there were no SCFP. This can occur in all eight directions.

Set-up (setup), firstly clears the ABM of anything from previous iterations (clear-all) and resets the time elapsed to zero (reset-ticks). It then loads the GIS libraries and imports the geospatial data (setup-gis): the raster DTM, the dimensions of the raster DTM, and the several population distribution shapefiles. It then calls the creation of the boundary (setup-boundary), this boundary shapefile ensures that at the end of every iteration the land returns to being land and the sea returns to being the sea. Whilst this subroutine does nothing directly, it provides a failsafe should the flood coding fail or an error to be produced, and ensures that the data is accurate. Finally, the set-up process applies the elevation values from the DTM to the cells (ask patches [set patch-elevation (gis:raster-sample elevation self)), anything below ECWL values and outside of the land boundary is then classed as the sea and coloured blue, with land coloured green. The ABM is now ready and is currently in $t = 0$, once the ABM is allowed to run it becomes 1991 and the population is applied.

Populate (populate?) is the second stage and is activated as soon as the ABM is allowed to run. Firstly, the process calls for the creation of the anti-boundary, a shapefile that covers the sea, this is to ensure errors are not produced within the ABM: the population distribution shapefile only covers the land, as that is where people live, however, during rasterisation this creates an error as rasters must be a quadrilateral. The anti-boundary handles this by instructing the ABM that cells within the sea have a population distribution of zero. Next the ABM checks if a decade has passed yet, if it has, it applies the new population share boundaries from that year (gis: apply-coverage census2001-dataset 'DISTRO' patch-distro). If the ABM gets to 2021, the process applies the 2021 population share but also gives cells a new value, patch-distrorate. The ABM then

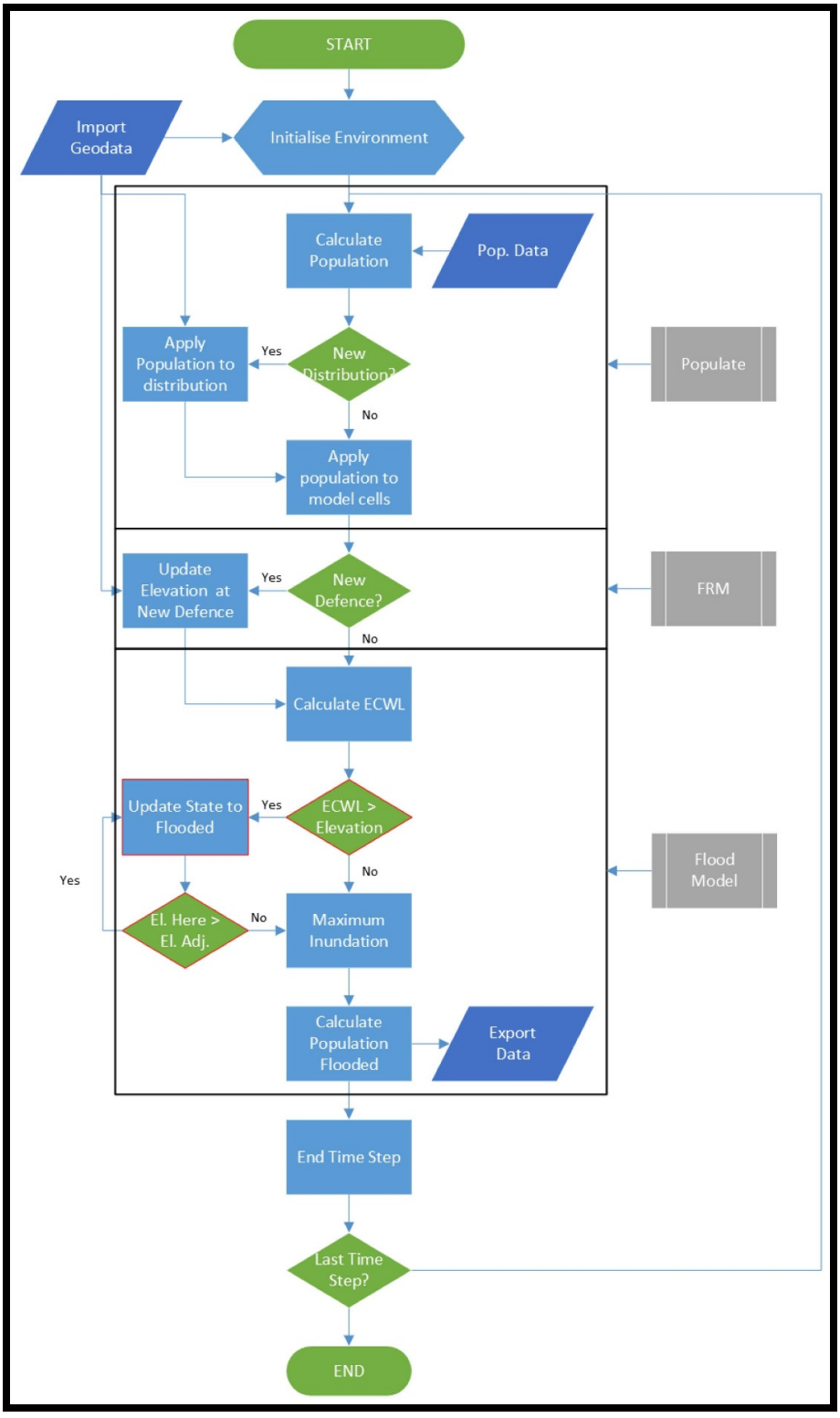

Figure 6. Flowchart of the ABM processes, starting from $t = 0$ to $t = 109$ yr, 1991–2100.

either applies this rate change and multiplies by the population, or uses the population share and then multiplies by the population as determined by whether it is before 2021 or after.

FRM (defend?) is the third process involved in the running of the ABM, involving two main steps in its operation. Firstly, the process checks whether enough time has passed and if the defence should be accounted for yet. If it has, the process calls the SCFP shapefile, a digitisation of the real-world defence. The process then adds the defence to the ABM, and instructs the underlying cells within its boundaries to change their

elevation based on the real-world height of the defence (ask patches gis: intersecting seawall [set patch-elevation defence height]).

In contrast, the Flood (flood?) process is the most complex; using bathtub flood modelling whilst also ensuring flood cell connectivity. The process checks sea cells if they have any land neighbours with an elevation less than the ECWL (ifelse any? patches with [(pcolor = blue) AND (any? neighbours with [patch-elevation < sea-level-flood AND pcolor = lime])]). Whilst this condition is TRUE, the subroutine repeats, with sea cells checking neighbouring land cells if their elevation is lower than the ECWL, if it is marking it *flooded*, and temporarily making it part of the sea. This repeats until there are no more land grid cells that can be flooded. Then once this subroutine cannot go any further, the ABM counts the squares that have been flooded and summates their populations (set output (sum [patch-population] of land with [pcolor = blue])), as determined by the population share shapefile and the Total Population equation. The ABM then checks if the operator has asked for an image of the maximum flooded extent of that year (export-images?), outputs one if so, and then progresses to the next year (tick).

Export (export?) forms the final stage of the ABM. This process ends the ABM once it reaches the year 2100, and exports the AfP and FA data collected from the ABM run as a .csv file, which can then be loaded into a spreadsheet and analysed.

2.2.2. Model validation

Validation was completed for Southport (figure 7), WSM (figure 8), and Portsmouth (figure 9). The Southport ABM produced an coefficient-of-determination (R^2) of 0.992 when comparing the Total Population produced by the model to the official ONS data (figure 7). Similarly, the WSM ABM had an R^2 of 0.998 (figure 8) and Portsmouth (figure 9) also had an R^2 of 0.992. However, the model of Total Population, for Portsmouth, for example, does not capture the small-scale peaks and troughs, and are therefore not represented by the ABM. Although, georeferenced population analysis revealed that changes in coastal population at these areas does not reflect the size of the natural variation within the ONS data. Therefore, these natural variations are not limited to SCFPs, but spread across the city, confirming that the ABM projects population well, and is validated in this regard.

The ABM was also validated for both the FA and AfP count model outputs. Using Portsmouth as an example, the Gamma flood model indicated that there are 4630 properties at risk of 1%AEP flooding at the baseline period, 2017 (Cantwell 2020). Using the 2.5 people per household assumption used in LFRMS (Local Flood Risk Management Strategy) modelling (Metropolitan Borough of Sefton Council 2014), this number of houses that would be translates to 11 575 people. The Portsmouth ABM simulation, when running on a 1%AEP event, produces an output of 11 234 people who are directly affected by flooding in 2017. Comparing the AfP output from the Gamma flood model to the one produced by the Portsmouth ABM gives the Portsmouth ABM an accuracy of 97% for 2017, confirming that the ABM simulates AfP reasonably well, and is validated in this regard.

One of the main drivers of AfP, determining whether a person will be flooded or not, is the coastal flood extent. To run the flood model, the ABM relies on an accurate DTM, a bare earth model of elevation derived from the Environment Agency, and accurate estimate of ECWLs derived using data from the Met Office. The ABM flood extent simulation uses a bathtub approach by comparing the elevation of a flooded cell to its eight adjacent cells, and if any of those cells are lower than those cells also become flooded. The bathtub approach tends to overestimate flooding due to a lack of connectivity (Kasmalkar *et al* 2023).

Nevertheless, the three ABM flood extent maps correspond well to that of the Environment Agency, and provides a good facsimile of flood extent in for Southport (figure 7), WSM (figure 8), and Portsmouth (figure 9). This is evidenced by the comparative maps, the similarity to the ONS projections and the good correspondence of the AfP output to that produced by the Gamma flood model, confirming that *the ABM simulates coastal flood extent reasonably well, and is validated in this regard.*

3. Results

This section presents the ABM socio-hydrological simulation outputs for the three case study sites: Southport, WSM, and Portsmouth.

3.1. Case study 1: Southport

The new defence at Southport was built in 2002 and provides a 150 yr Standard of Protection (SoP), protecting against a 0.66%AEP event in 2002. The topography of the landscape is presented in figure 10.

Before the construction of the SCFP in Southport, as the ECWL increases, the AfP decreases (figure 11), while the FA remains stable (figure 12). The construction in 2002 led to a sharp decrease in AfP (figure 11) and FA (figure 12), the magnitude of this decrease is represented by the steep fall in the AfP derivative

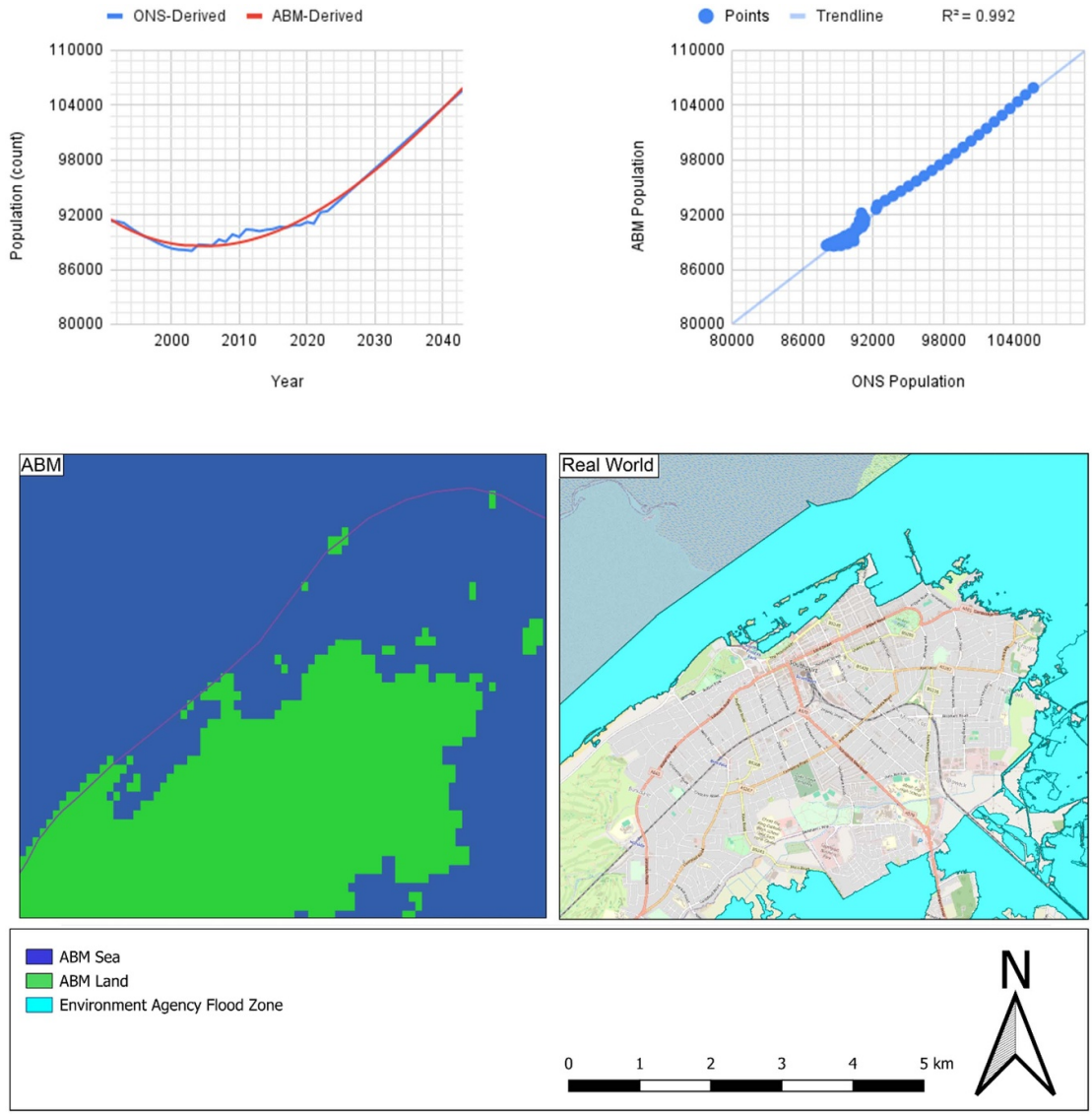

Figure 7. Comparison of the ONS and the modelled population data used within the Southport ABM and a scatterplot representing the ABM-derived compared to the ONS-derived population data for Southport with *R*-squared value of 0.992. The maps demonstrate the flood extent of a 0.1%AEP scenario output from the ABM and the floodable area determined by the Environment Agency (EA) for Southport.

(figure 13). The negative derivative output demonstrates a decreasing gradient in AfP, that quickly reverts to zero in the following year: it is clear that the construction of the new SCFP had a positive impact on AfP, as would be expected.

After the introduction of the new SCFP, Southport population behind the new defence starts increasing, followed by a steady increase in the AfP, AfP recovering to pre-defence levels by 2045. Afterwards, AfP mirrors the growth in Total Population until around 2086 (figure 11), at which point the growth rate stabilises (figure 13). In spite of increasing ECWL (figure 11), growth in the FA of Southport also slows down and eventually stabilises in the 2050s (figure 13). The elevation of Southport is predominantly <5 m above sea level (figure 10), and this land is mostly flooded even after the construction of the new SCFP, with FA decreasing to its lowest of 60% after the defence, and its highest 78% in 2100 (figure 12). This is an example of diminishing returns: the higher elevated places are the less likely to flood, and so would require much higher ECWL, hence the slowdown in AfP around this period (figures 11 and 13).

In 2085 the SCFP crest height will be exceeded (unless upgraded) by the ECWL, flooding the low-lying areas previously defended. AfP increases dramatically as some locations become floodable, whilst they were not before, this leads to a rate of increase far greater than the growth of Total Population (figure 11) and a large increase in FA (figure 12). This sudden high-level growth is also represented as a large increase in the AfP derivative (figure 13), jumping to over 33 033 yr^{-1}, far greater than the 15 585 yr^{-1} people initially protected by the construction: the SCFP becoming exceeded led to an extra 17 448 people now directly

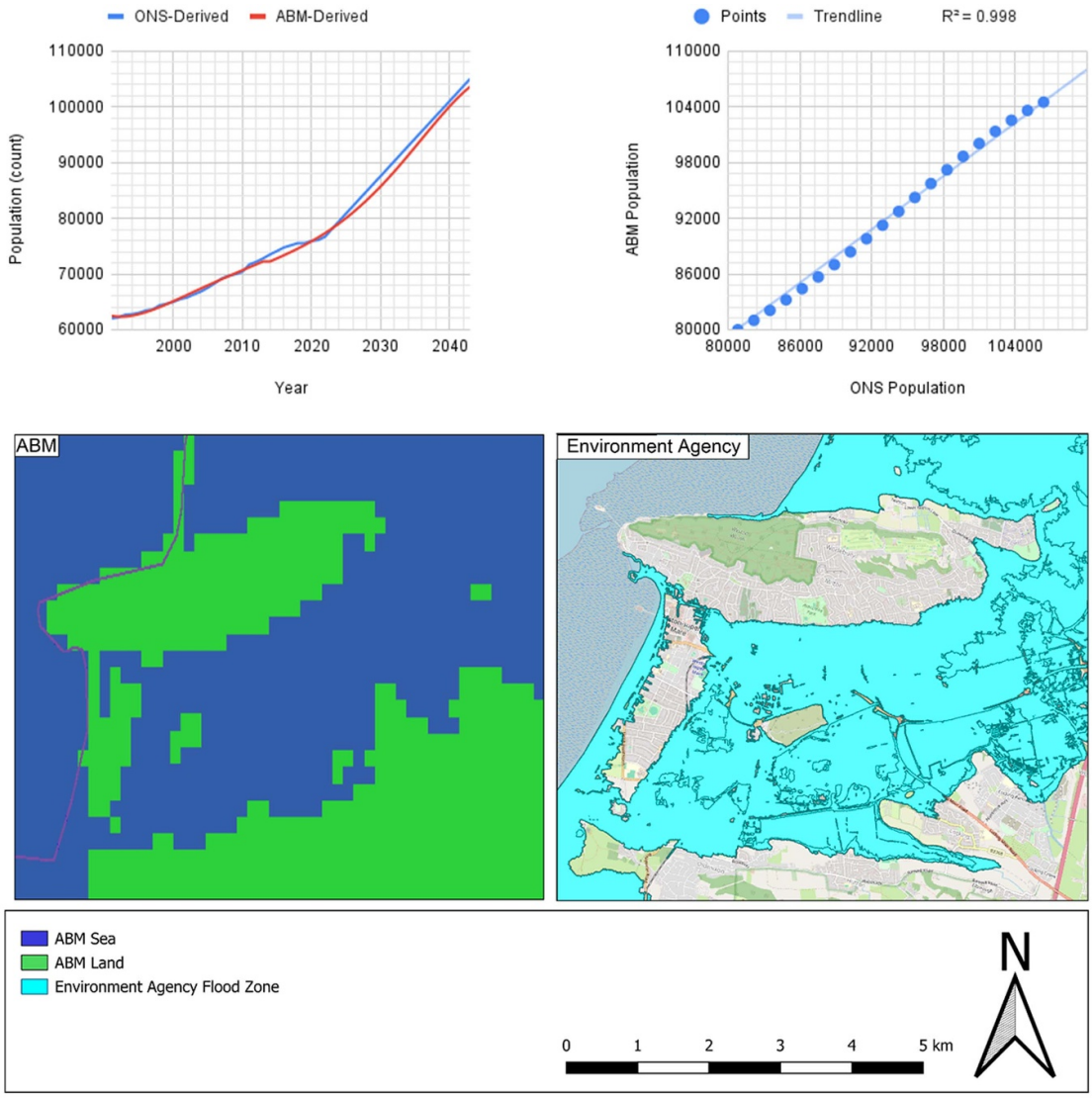

Figure 8. Comparison of the ONS and the modelled population data used within the Weston-super-Mare ABM and a scatterplot representing the ABM-derived compared to the ONS-derived population data for Weston-super-Mare with *R*-squared value of 0.998. The maps demonstrate the flood extent of a 0.1%AEP scenario output from the ABM and the floodable area determined by the Environment Agency (EA) for Weston-super-Mare.

affected by flooding (figure 14). These populations protected by the SCFP would not have been flooded during the 2002–2085 period and would therefore have limited experience with flooding, decreasing flood awareness and preparedness, putting them at a high level of risk. It is unlikely that new urban development would have been sanctioned in the area where new buildings were built in Southport following the new SCFP construction, and that these new populations would have moved there, had it not been built (Department for Communities and Local Government 2012). Moreover, due to the increase in ECWL between the 2002 and 2085 period (figure 11), when the SCFP is exceeded, low lying areas that had not been flooded previously would now be floodable (figure 14), without flood risk communication, these populations would not be prepared for such an event. *Therefore, the short-term savings provided by the construction of the new SCFP in Southport would be greatly overshadowed by the long-term losses, highlighting the importance of considering these unintended consequences in future coastal FRM and spatial planning.*

3.2. Case study 2: WSM

The new SCFP at WSM was finished in 2011 and provides a 200 yr SoP (i.e. providing protection against a 0.5%AEP event in 2011). The topography of the landscape in figure 15.

Before the upgrading of the new defence in WSM, with a steady increase in ECWL (figure 16), AfP also increases steadily by 3 yr^{-1} (figure 16), while the FA remained stable (figure 17). The upgrading of the SCFP in WSM led to a decrease in AfP by 78 people, FA by 0.8% (figure 17), and the derivative of AfP (figure 18). The decrease in AfP per year is too few to be apparent in the graphs due to the large AfP increase when the

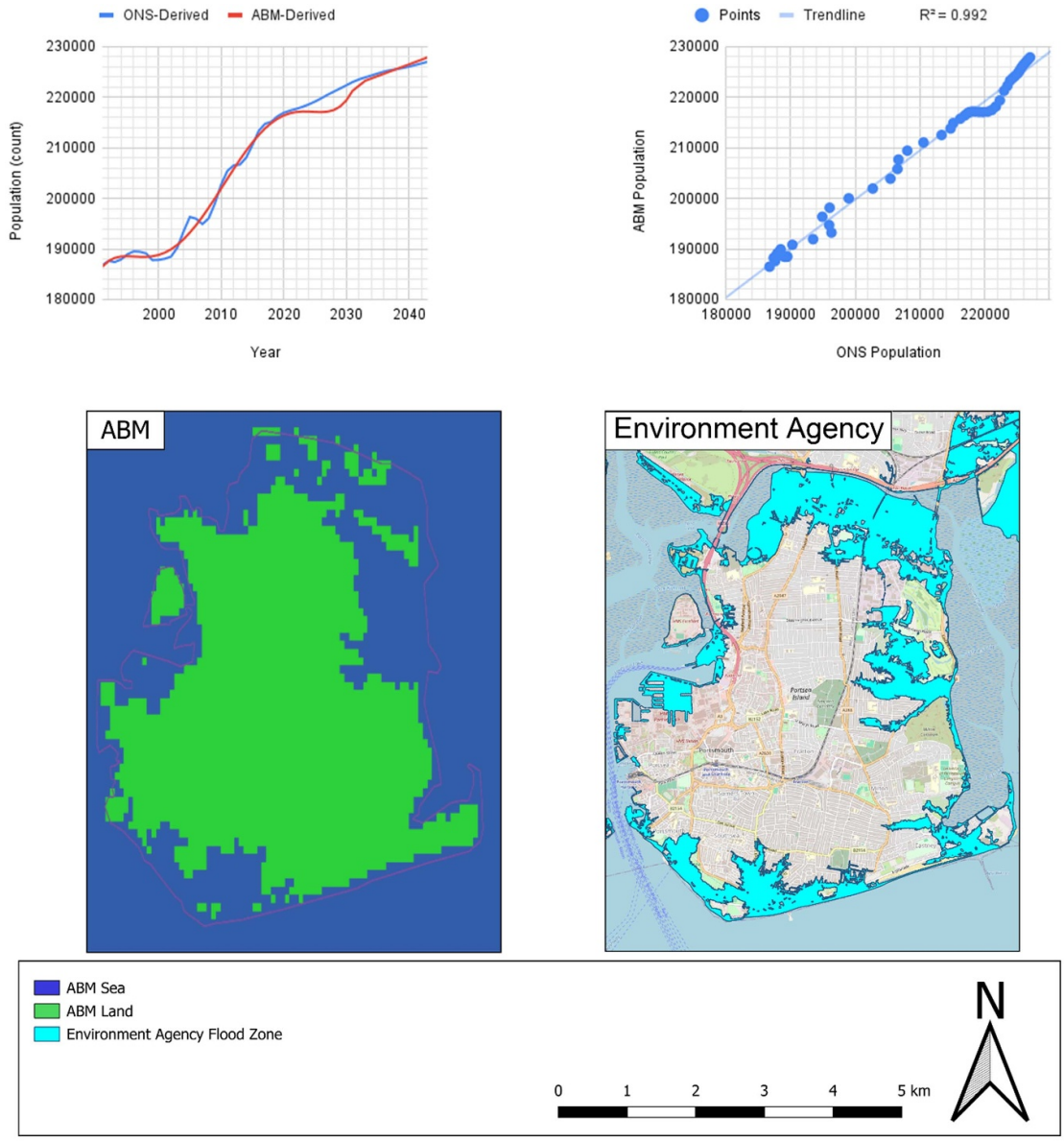

Figure 9. Comparison of the ONS and the modelled population data used within the Portsmouth ABM and a scatterplot representing the ABM-derived compared to the ONS-derived population data for Portsmouth with *R*-squared value of 0.992. The maps demonstrate the flood extent of a 0.1%AEP scenario output from the ABM and the floodable area determined by the Environment Agency (EA) for Portsmouth.

ECWL becoming higher than the crest height of the SCFP and a flood occurs. This is due to the fact that WSM already had a mostly effective SCFP, protecting not only itself but also the North Somerset Levels behind with an upgrade to a 1-in-200 yr SoP from a 1-in-50. If there was no other SCFP present, then the decrease in AfP would likely be much greater.

Following the upgrading of the SCFP in WSM, the AfP derivative quickly returns to around 2 yr^{-1} steadily increasing to 6 yr^{-1} before the defence is exceeded in 2054 (figure 18); although, there are several smaller peaks in the run up to it being exceeded: a temporary increase to 18 yr^{-1} in 2026, 12 yr^{-1} in 2046, and 25 yr^{-1} in 2048. These slight increases in the AfP derivative are most likely driven by the interaction between the ECWL and the underlying DTM raster data, which has several smaller frequency peaks between 0 m and 5 m (figure 15), these interactions also translate to the slight increases in FA across this period (figure 17). Moreover, changes in population distribution attributed to the SCFP upgrades may have led to increases, and decreases, in both, AfP and its derivative.

Following this period, there was a very steady increase in the AfP of WSM, which recovers to pre-upgrade levels by 2031 (figure 16). The SCFP led to a decrease in FA from 5.0% to 4.1% the year after (figure 17). However, once the SCFP is exceeded, the FA increases from 4.3% to 54.2% in a single year, rising to 56.5% by 2100 (figure 17). The upgraded SCFP in WSM is exceeded in 2054 under the ECWL scenario explored,

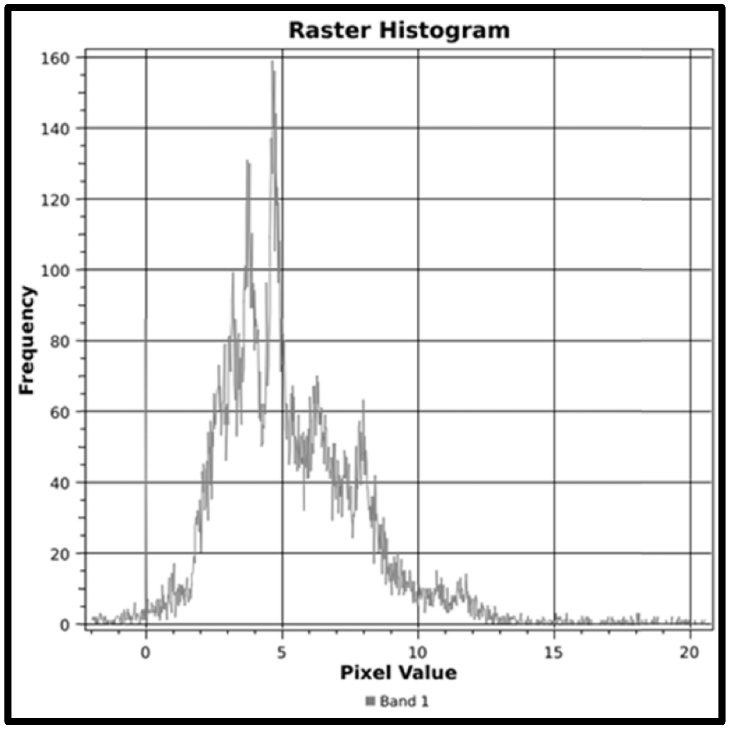

Figure 10. Raster histogram based on the DTM data used in the Southport ABM.

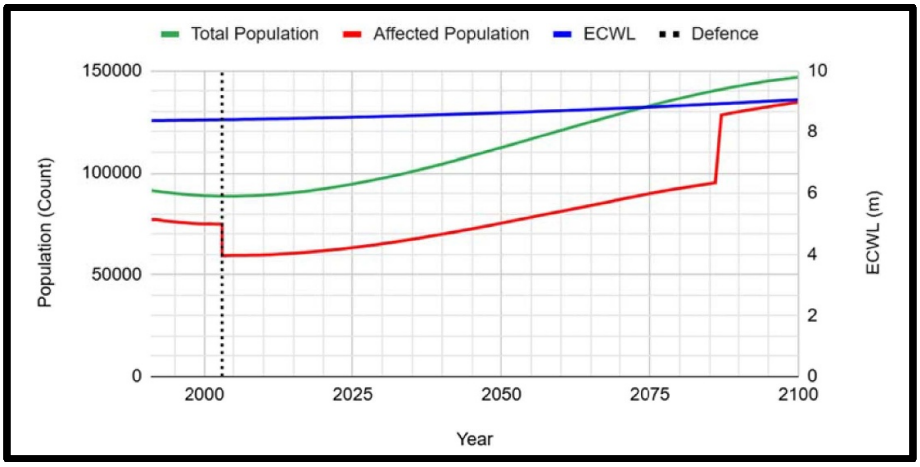

Figure 11. Total Population, Affected Population, and ECWL with a 0.1% AEP under the RCP8.5 scenario with waves.

flooding low lying areas previously defended by it (figure 19), and new land that had never been flooded before due to higher ECWLs than had hitherto never been experienced. AfP (figure 16) and FA (figure 17) increases drastically. This sudden increase in AfP translates to a large increase in its derivative (figure 18), jumping to 26 008 yr^{-1}, far greater than the 78 yr^{-1} protected when the defence was initially upgraded. The upgraded SCFP in WSM being exceeded leads to an extra 25 930 people being directly affected by coastal flooding than before the defence was upgraded (figure 19). These populations would have limited experience with flooding, and this would likely impair flood awareness, preparedness, and consequently responsiveness. This highlights the importance of flood risk communication, so that when large-scale inundation events do occur, the population is ready and capable. *Therefore, the short-term savings provided by the upgrading of the SCFP in WSM would be greatly overshadowed by the long-term losses, highlighting the importance of considering these unintended consequences in future coastal FRM and spatial planning.*

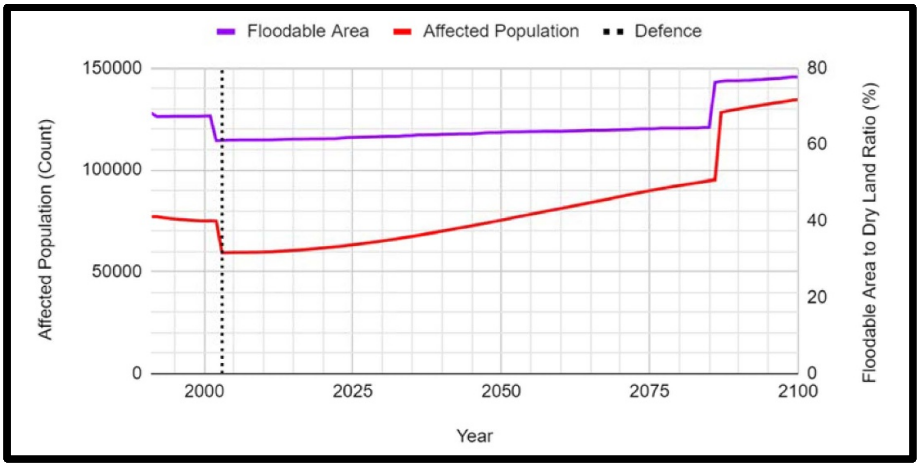

Figure 12. Ratio of dry land to wet land (FA) and population directly affected by flooding with a 0.1% AEP under the RCP8.5 scenario with waves.

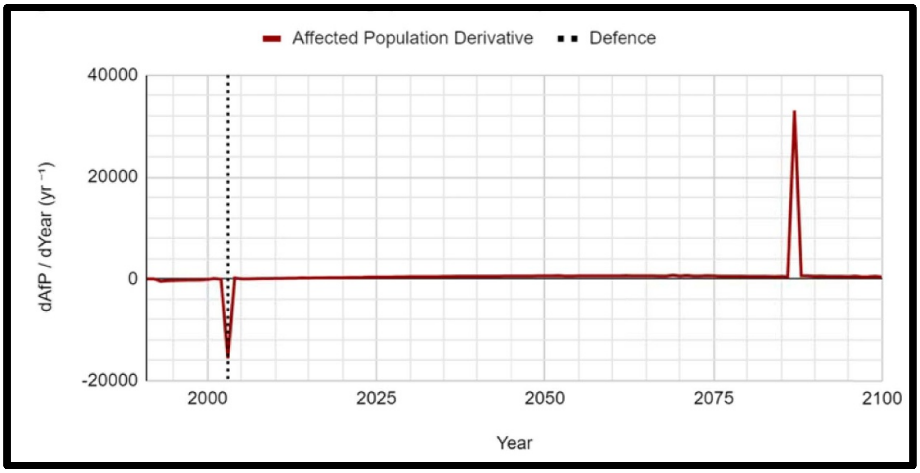

Figure 13. Derivation (dAfP/dYear) of the population directly affected by flooding with a 0.1% AEP under the RCP8.5 scenario with waves.

3.3. Case study 3: Portsmouth

The defences at Portsmouth were constructed in multiple phases or upgraded multiple times over the decades: Old Portsmouth site in 2005, NPCS (North Portsea Coastal Scheme) Phase 1 in 2015, NPCS Phase 2 in 2016, NPCS Phase 3 in 2019, as well as the ongoing Southsea scheme starting in 2022 and finishing in 2029. Some defences were yet to be built, and information from these came from planning documentation, these include NPCS Phase 4 (2024), NPCS Phase 5 (2026), and subsections of the Southsea scheme. The six sub-projects of the Southsea projected have not been represented in the charts below for better visualisation, but are represented by the final Southsea line graph (2029) which connects the project together. The topography of the landscape in figure 20.

Before the Old Portsmouth SCFP, AfP in Portsmouth was initially flat, then increased year-on-year up to the construction (figure 21). Following the completion of the Old Portsmouth SCFP in 2009, AfP (figure 21), FA (figure 22), and the derivative of AfP (figure 23) all showed decreases, amounting to a fall of 421 yr^{-1}. However, the overall amount of AfP increased again to that of before the Old Portsmouth coastal defence, due to coastal flooding in other unprotected areas of the city (figure 21), confirmed by a continuous rise in FA of the city after the initial decrease (figure 22).

During the period following the Old Portsmouth SCFP and NPCS Phase 1 there was an increase in AfP, increasing exponentially with the AfP derivative not only remaining positive, but increasing (figure 23). Whilst FA did increase over this period, the rise was steady, whereas the citywide Total Population rose at its greatest rate (figure 22) and was therefore the most likely primary driver of AfP growth over this period, negating decreases in AfP caused by SCFPs. Then, as NPCS phases continue, AfP remained relatively stable, oscillating between positive and negative growth, with Phase 3 leading to a 341 AfP decrease (figure 23). This

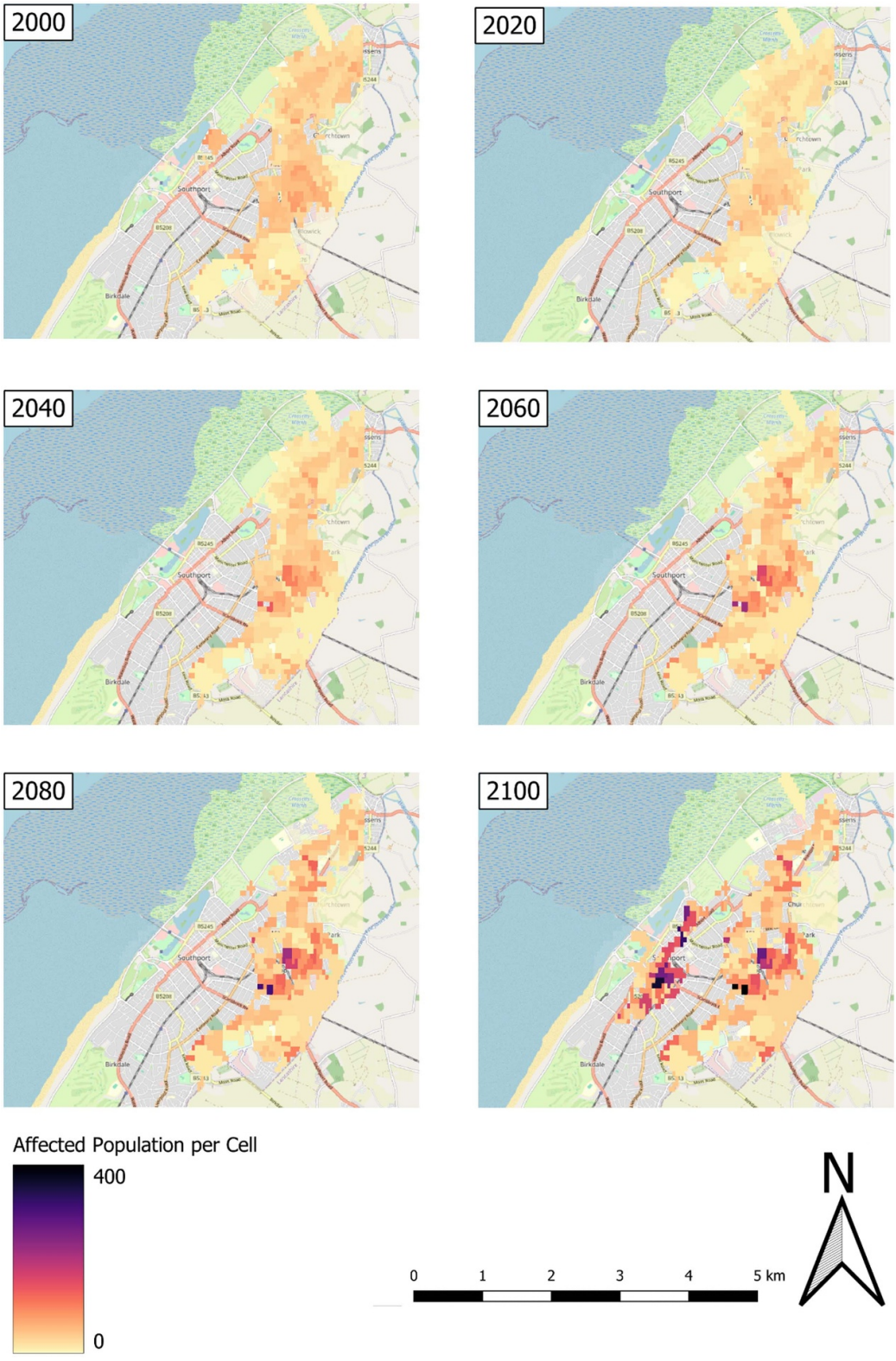

Figure 14. ABM simulation of the spatial distribution of AfP in Southport across the century.

phase directly protected the north-west of Portsea Island and did not see a Total Population decrease over this period, implying that the large decrease is associated with the SCFP being implemented. The NPCS was designed to operate at its best together, and therefore linking with already implemented phases would also provide greater flood protection and impact reduction.

The completion of the NPCS Phase 5 and Southsea scheme saw the greatest reduction in AfP (figure 21), with a decrease of 7200 yr^{-1} (figure 23). Then, once the Southsea scheme had been completed, there was an

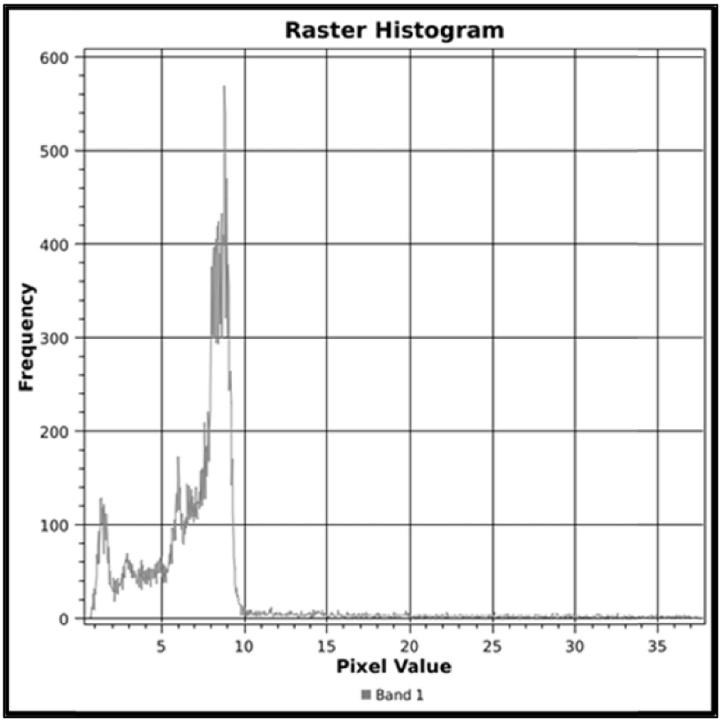

Figure 15. Raster histogram based on the DTM data used in the Weston-super-Mare ABM.

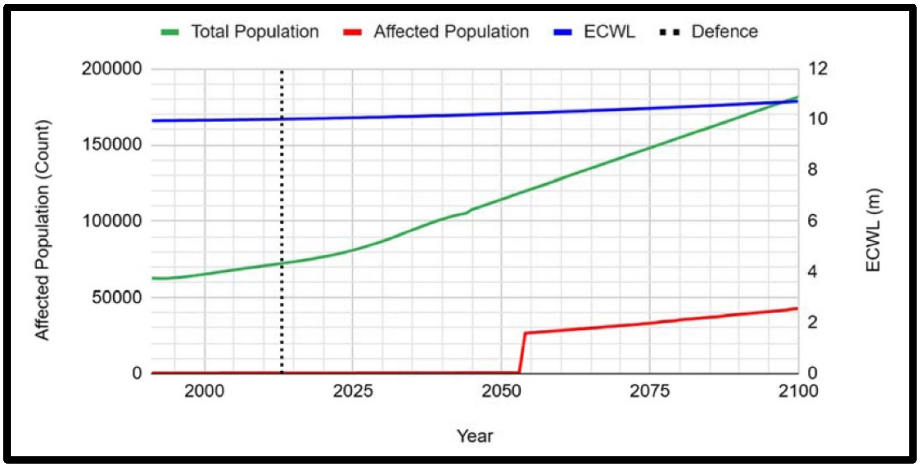

Figure 16. Total Population, Affected Population, and ECWL with a 0.1% AEP under the RCP8.5 scenario with waves.

even greater decrease of 8807 yr^{-1} (figure 23). However, the completion of the NPCS Phase 5 scheme led to the greatest decrease in FA, decreasing by 11.4%, from 26.7% to 15.3%, compared to a decrease of 3% from the Southsea scheme (figure 22). This suggests that Southsea is a much more populated area than north Portsmouth, where the NPCS protects. Moreover, this is concordant with the idea that the area protected by the NPCS is primarily industrial with limited residential population and that the unintended consequences of SCFPs can be affected by land availability for residential growth (Fusinato *et al* 2024).

Following the large decrease in AfP and FA in Portsmouth, both factors remain comparatively low, with minimal growth rate: AfP growth remains around 4 yr^{-1} (figure 23). This continues up until 2067 at which point AfP increases by 137 yr^{-1}, and is the last spike before the significant increase later towards the end of the century (figure 23). These increases begin as the ECWL exceeds the SCFP crest height (figure 21) and inundating areas with higher elevations, less frequent than those around the 4 m mark (figure 20). The SCFPs are first exceeded significantly in 2083, and despite the FA only increasing by 0.4% (figure 22), there is a 2581 increase in AfP (figure 23), suggesting a densely populated area had become flooded, the city centre, as the Old Portsmouth defence being exceeded (figure 24). As time progresses such instances become more

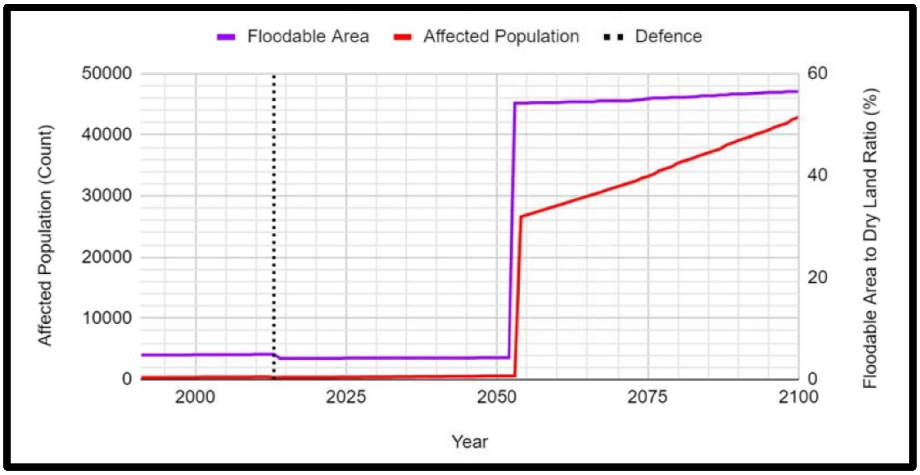

Figure 17. Ratio of dry land to wet land (FA) and population directly affected by coastal flooding with a 0.1% AEP under the RCP8.5 scenario with waves.

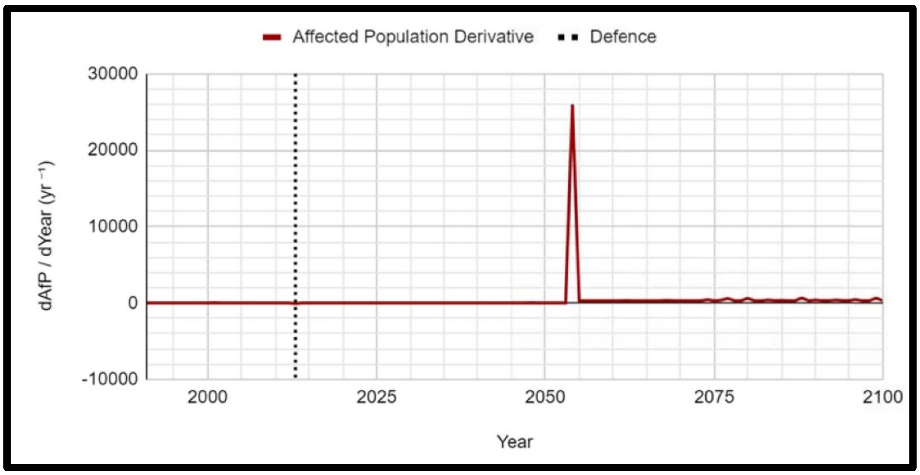

Figure 18. Derivation (dAfP/dYear) of population directly affected by coastal flooding with a 0.1% AEP under the RCP8.5 scenario with waves.

common with the next major one being in 2091, with an increase of 759 people who are directly affected by flooding (figure 23) and an increase of 0.3% in FA (figure 22). After this, there was an increase of 1533 people who were directly affected by flooding, and a corresponding increase of 0.9% in the FA. This matching increase in FA was triple the 2091 increase, despite having double the population; this reflects the sizable variance within the underlying DTM in Portsmouth (figure 20). The final large increase in AfP occurred not too long after in 2097 when the ABM projected an increase of 652 people in the AfP output (figure 23) and a corresponding 0.2% increase in FA (figure 22).

AfP (figure 21) and FA (figure 22) outputs never returned to the levels of before Old Portsmouth. Moreover, the decreases in AfP caused by the construction of the NPCS Phase 5 and Southsea SCFPs were much greater than any of the increases in dAfP/dt generated by the ECWL rising to higher than the crest height of any of the SCFPs (figure 24). Although, if the ABM were to run for longer, this may become apparent. Exploratory ECWL scenarios beyond 2100 are available, but they are of less statistical certainty than those used up to the end of the twenty-first century. The NPCS protected the northern part of Portsea Island, an area dominated by industry; this led to limited change in AfP per phase, until the completion of the fifth phases of the project that linked the project together. However, the change in FA compared to the change in AfP for NPCS Phase 5 reflects the low population density of the area, and suggest a strong link between the impacts of SCFPs and the land use of the local area. Moreover, as demonstrated by census and LiDAR change data, there was limited change in the residential area by the NPCS Phase 1 SCFP, this may also indicate an upper capacity limit that would also influence the impacts of SCFP, and hence there was no statistically significant difference in the change in population distribution. *Therefore, to summarise, the*

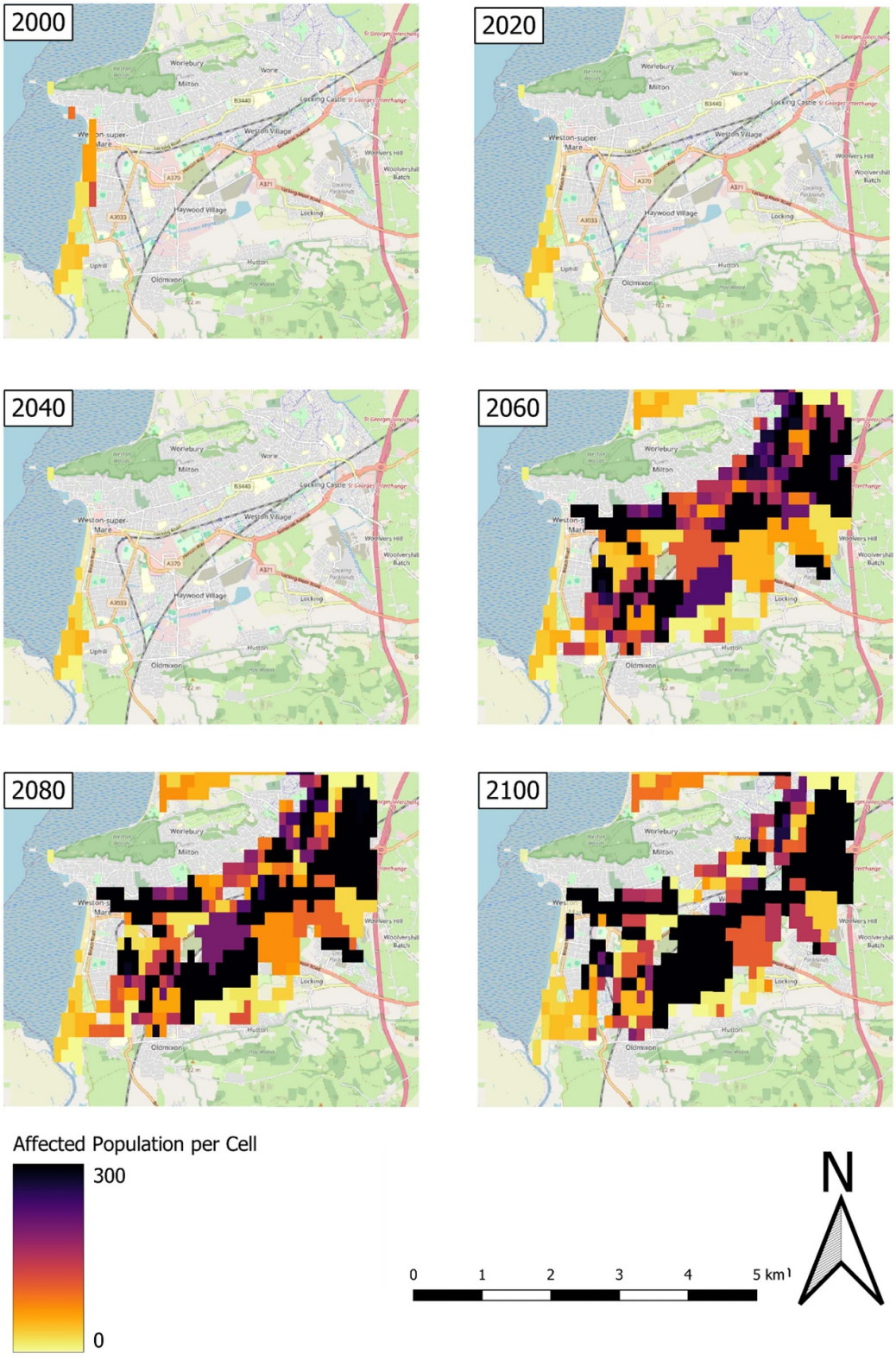

Figure 19. ABM simulation of the spatial distribution of AfP in Weston-super-Mare across the century.

overall effect of the combined SCFP schemes in Portsmouth meant that AfP did not increase back to levels prior to the completion of the Old Portsmouth SCFP. The repeated SCFP schemes limited inundation, and pre-existing land use and urban development reduced potential socio-economic impacts.

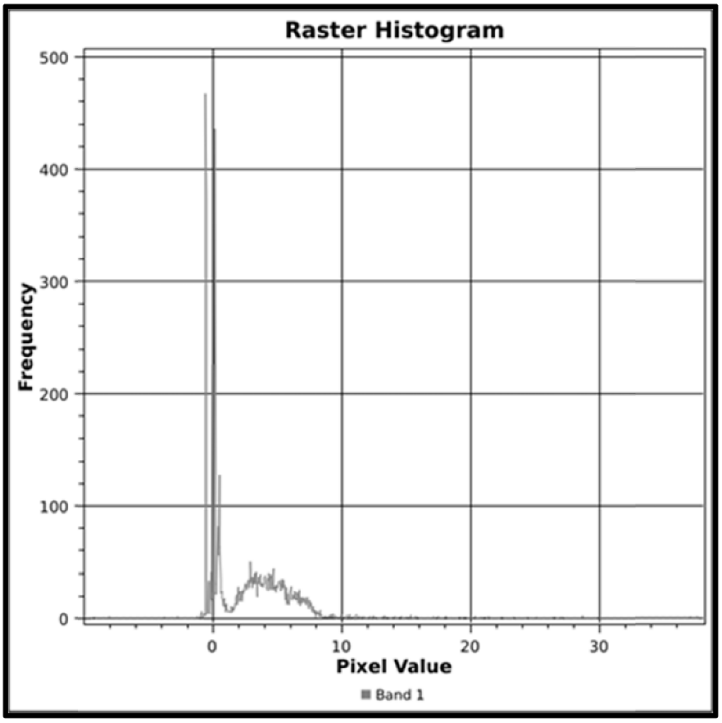

Figure 20. Raster histogram based on the DTM data used in the Portsmouth ABM.

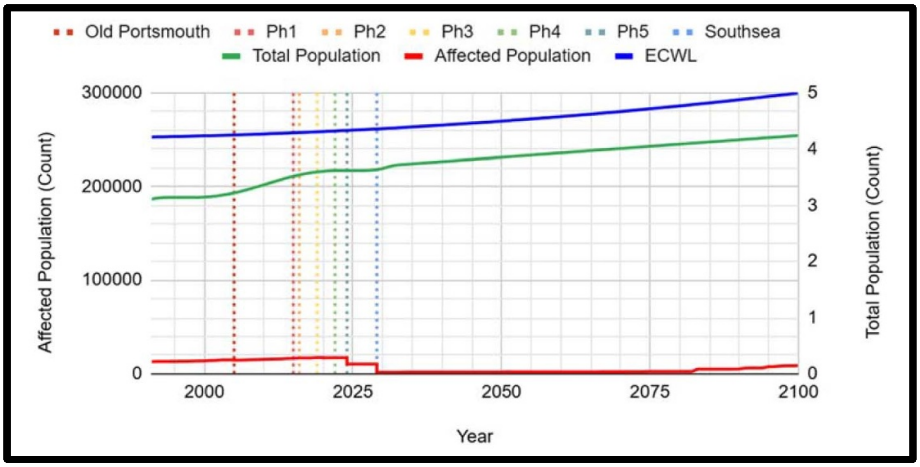

Figure 21. Total Population, affected population, and ECWL with a 0.1% AEP under the RCP8.5 scenario with waves.

4. Discussion & conclusion

ABM of the socio-hydrological processes at the SCFP demonstrated clear emergent phenomena. The results suggest that during a Latency phase (figure 25), population would continue to increase behind the SCFP whilst the ECWL continues to increase. This would continue until the ECWL exceeds the SCFP crest height and, in locations with flatter topography (such as in WSM, figure 19), the flood extent would reach a far greater area than before, visible in the spatial AfP mapping and demonstrating the utility of SCFPs. The combination of an increased settlement behind the SCFP and a larger flood extent would see a far greater proportion affected by the flooding than when the defence was initially built, leading to the large ΔAfPs. From the lack of past flooding experience would be less prepared in the event of low-frequency, high-impact flooding (Ridolfi *et al* 2021), an event exacerbated by the SCFP which limits higher-frequency, lower-impact inundations (Haer *et al* 2020). Notably, when flood risk is covered collectively, such as by a flood insurance scheme, population growth in floodplains is substantially higher than where insurance reflects individual

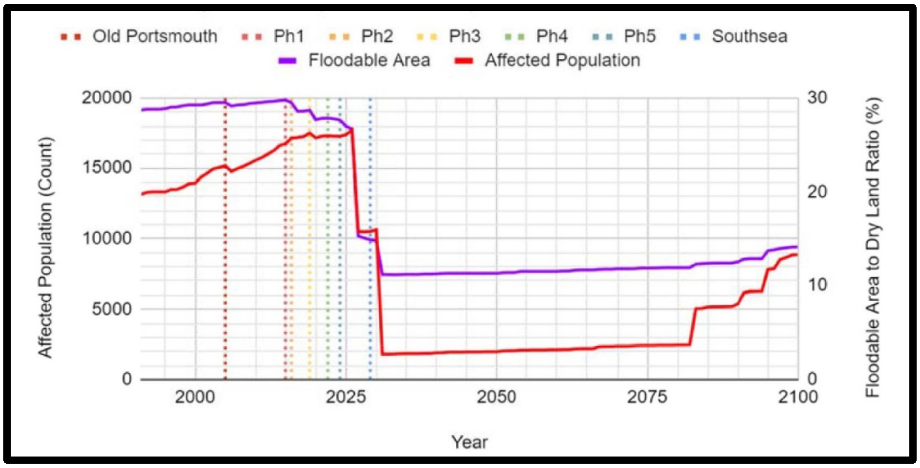

Figure 22. Ratio of dry land to wet land (FA) and population directly affected by coastal flooding with a 0.1% AEP under the RCP8.5 scenario with waves.

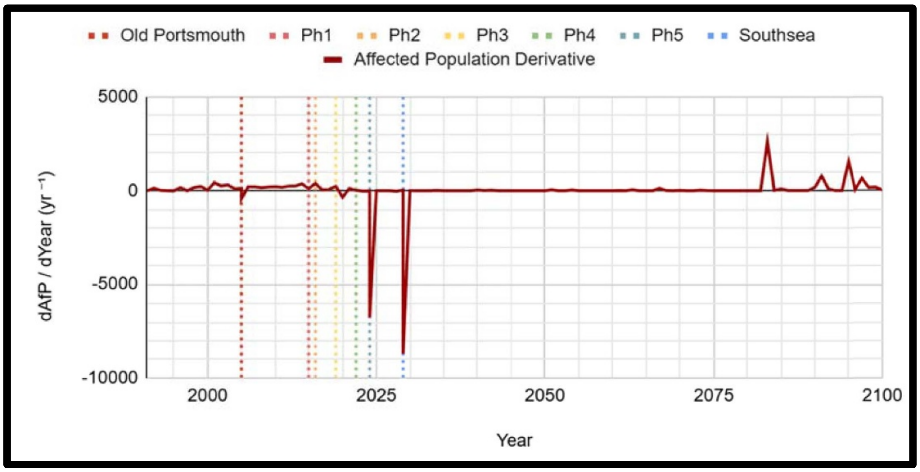

Figure 23. Derivation (dAfP/dYear) of the population directly affected by coastal flooding with a 0.1% AEP under the RCP8.5 scenario with waves.

household risk, leading to accelerated increases in long-term flood exposure (Tesselaar *et al* 2023), these processes could be integrated into the ABM in future studies.

Consequently, there is a clear pattern on the implications of SCFP on socio-hydrological processes, which can be broken down into five stages (figure 25):

- **Stage 1: Design**
  During this stage the SCFP is being designed and has not yet been implemented. AfP is affected by both the extent of coastal flood inundation and natural population changes.
- **Stage 2: Implementation**
  This stage references the construction (or major upgrade) of the SCFP and a dramatic decrease in AfP driven by a decrease in the ability of coastal flooding to permeate deeply into the settlement.
- **Stage 3: Latency**
  During this period, population increases behind the newly constructed (or majorly upgraded) SCFP. Meanwhile, ECWL remains lower than SCFP crest height thus AfP sees little change outside of natural population change.
- **Stage 4: Flood**
  This stage sees the SCFP being exceeded by higher ECWL scenarios and flooding the settlement behind it. AfP increases dramatically as coastal flooding becomes a large driver of it again. Due to increases in ECWL, coastal flooding travels further and affects populations at higher elevations of the town than it was able to previously.

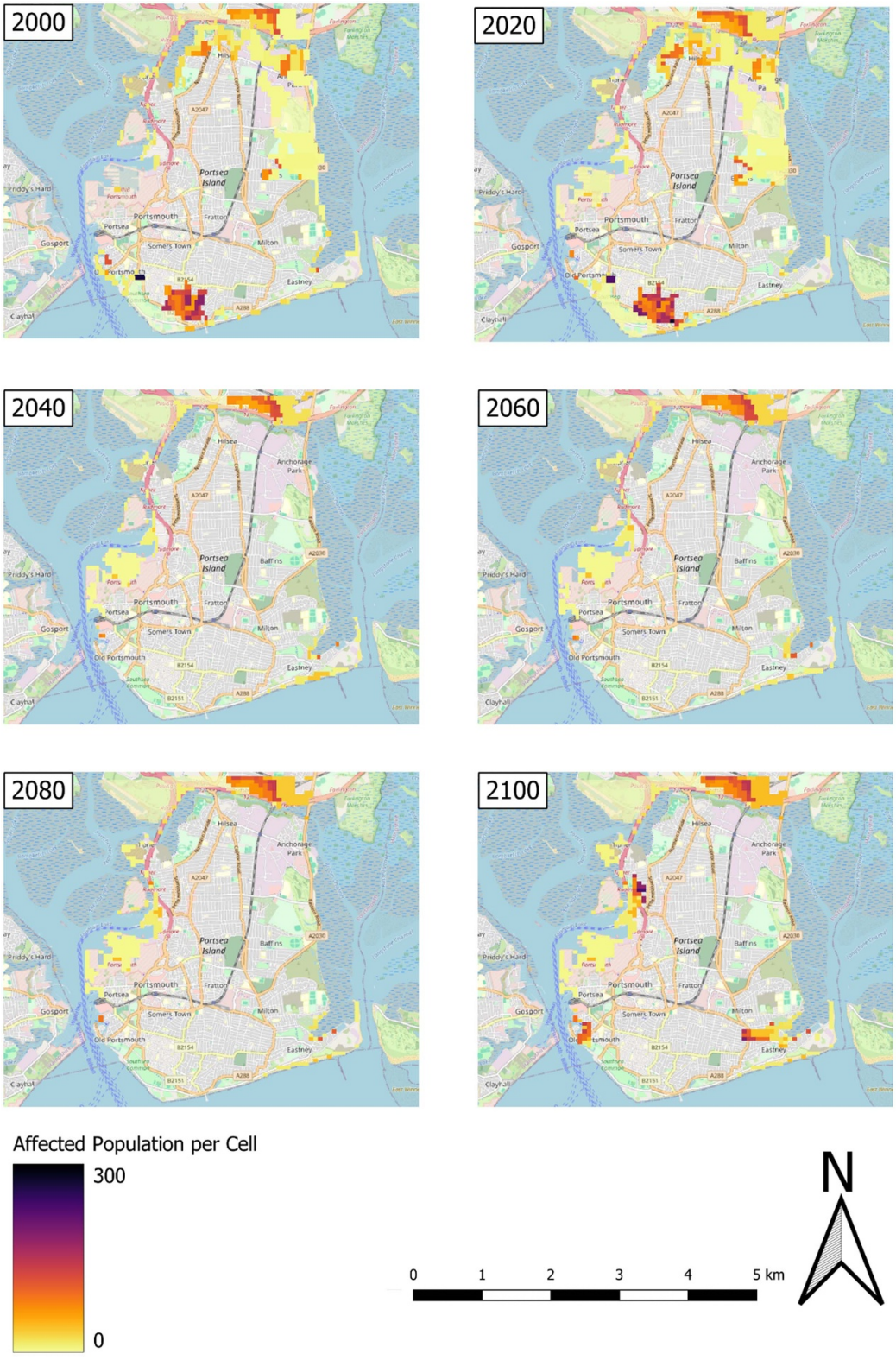

Figure 24. ABM simulation of the spatial distribution of AfP in Portsmouth across the century.

- **Stage 5: Post-Flood**
  This is the final stage and presents the new normal following Stage 4, which now occurs regularly as the ECWL remains higher than the defence itself (unless upgraded inline with the increase in ECWL). AfP again returns to being driven by both the extent of coastal flood inundation and population changes, both, spatially and fundamentally.

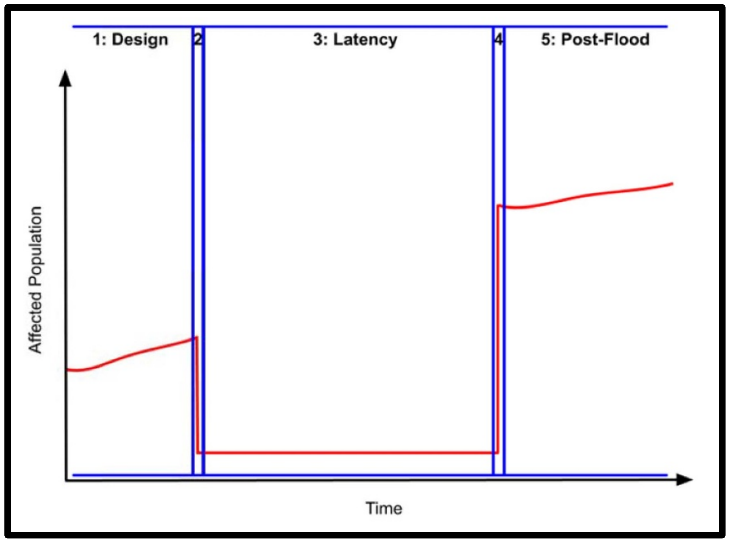

Figure 25. Conceptualisation of the socio-hydrological processes in a hypothetical town before, during, and after a SCFP was constructed (or majorly upgraded) and a resulting flood once ECWL was greater than the SCFP crest height.

In Southport the SCFP initially reduced the AfP, but over time this protection led to a greater ΔAfP when the ECWL exceeds the SCFP crest height due to increased settlement behind the SCFP (as in Di Baldassarre *et al* 2018). This pattern again aligns with the SDP, leading to increased exposure once SCFP are overwhelmed (as in Ludy and Kondolf 2012). WSM showed a larger ΔAfP once the ECWL exceeds the SCFP crest height as many areas were already defended by a seawall. This echoes findings from Hurricane Katrina whereby the failure of the levee system resulted in disproportionately high impacts on populations who believed they were safe (Burby 2006, Gotham *et al* 2018). The combination of these factors would therefore likely cause a structurally proactive FRM authority to further enhance SCFP, renewing the SDP. Portsmouth, on the other hand, demonstrated that with limited residential development around the NPCS, the role of the SCFPs in shaping population socio-spatial dynamics is diminished, illustrating again how land use can moderate the socio-hydrological impacts of SCFPs in densely populated and highly developed areas, such as Portsmouth (as in Fletcher 1992).

Therefore, the study identified two critical pathways that inhibit coastal population growth and development occurring due to local increases in SCFP. These are, in sequence, *Land-use Drive*n and *Population Driven* (figure 26):

1. Land-use Driven
This represents the case where pre-existing use of land, whether used for industrial, commercial, or residential purposes. For example, if exiting land use is non-residential, then population increase cannot occur.

2. Population Driven
This represents the case where an already very high population density limits further population increases, either due to the economics of supply and demand in the area, or physically limits the number of people that can live in the area.

The findings of this study, combined with those of others (e.g. Haer *et al* 2020), suggest that there is an intangible risk measure that increased from an upgrade compared to the initial construction, which would then suggest a cyclicality. The Portsmouth ABM further exemplified this with the appearance of the inhibition pathways. These pathways mitigate the unintended impacts of newly constructed, or upgraded, SCFPs, and from the ABM simulation it became apparent that pre-existing land use or high-density population can limit growth in population during the latency period and therefore minimise the absolute change in AfP from before the SCFP was constructed to the time that the ECWL exceeds the SCFP crest height.

However, there are also some limitations associated with using ABMs, one of the main challenges is the complexity of model calibration and validation, particularly when incorporating multiple interacting factors (Sun *et al* 2016). Ensuring that the ABM accurately represents real-world processes and behaviours requires extensive data collection and validation, which can be time-consuming and resource-intensive. Additionally, overcomplicated ABMs may unintentionally introduce uncertainty and bias (Smajgl *et al* 2011), reduce the

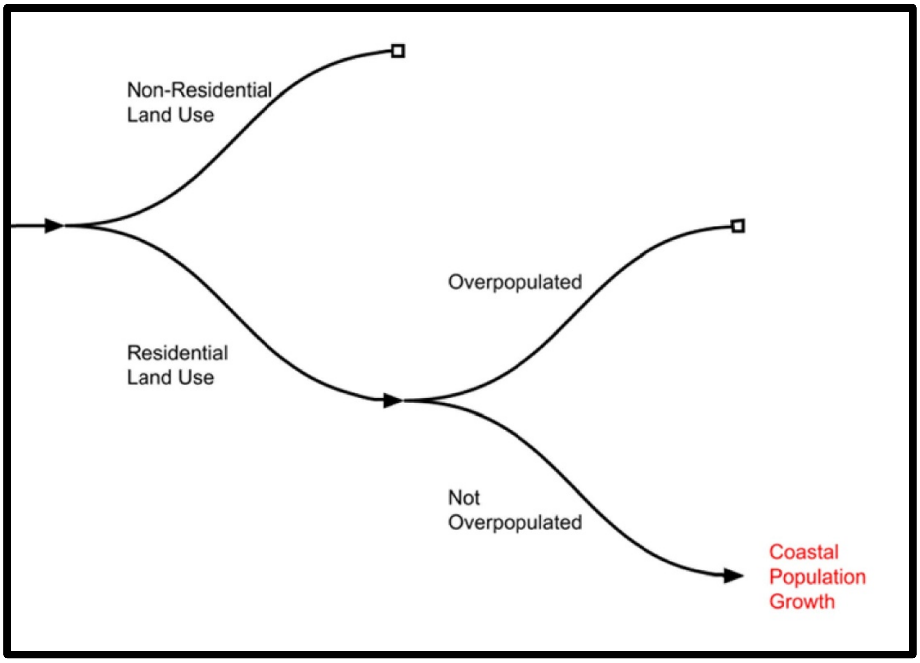

Figure 26. Conceptualisation of the inhibition pathways that hinder the coastal population growth during the latency period as an unintended consequence of SCFP.

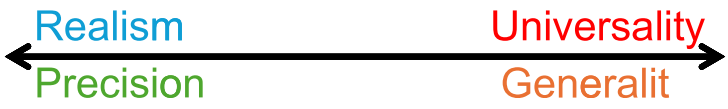

Figure 27. Trade-offs in model construction between precision, realism, and generality.

ease of use and evaluation (Müller *et al* 2014), and can also lead to potential difficulties in analysing multidimensional data and outputs (Lee *et al* 2015, Sun *et al* 2016).

ABMs do provide a method of simulating emergent phenomena by replicating behavioural patterns (Bonabeau 2002). However, in pursuit of being realistic they often require many parameters, inevitability becoming more complex, and so move away from comprehensibility and transparency (Dubbelboer *et al* 2017), becoming less generalizable (Janssen and Ostrom 2006). To maintain precision, realism may be sacrificed to produce a more generalised model, applicable in a wider range of case studies, yet losing its tangibility. Whereas sometimes generality is lost to focus on accurate predictions for specific case studies (Troy *et al* 2015). In developing the ABM, it was necessary to balance precision, realism, universality, and generality by calibrating model parameters based on best publicly available data, whilst ensuring that the model remains sufficiently generalizable across different study areas. These trade-offs are demonstrated in figure 27, and represent the decisions that must be made in order to replicate reality in some form. Model calibration and validation were used to progress the model towards becoming more precise and realistic, this was balanced against generality by ensuring that no new local-specific subprocesses were added, and that the script was universal.

Despite these challenges, ABM remains a valuable tool for exploring socio-hydrological processes and associated emergent phenomena, and assessing the impacts of SCFPs under future climate scenarios. By integrating socio-spatial and environmental dynamics and institutional factors, ABMs have the ability to inform more robust and adaptive coastal management strategies for building resilience to coastal flooding (Erdlenbruch and Bonté 2018, Haer *et al* 2020).

Data availability statement

The data cannot be made publicly available upon publication because no suitable repository exists for hosting data in this field of study. The data that support the findings of this study are available upon reasonable request from the authors.

Acknowledgments

This research was funded by the EPSRC Grant Number EP/T518116/1.

ORCID iDs

Morgan J Breen https://orcid.org/0000-0002-5733-1762
Abiy S Kebede https://orcid.org/0000-0002-7844-1151
Carola S König https://orcid.org/0000-0002-9289-3154

References

An L 2012 Modeling human decisions in coupled human and natural systems: review of agent-based models *Ecol. Modelling* **229** 25–36
Andreadis K, Wing O, Colven E, Gleason C, Bates P and Brown C 2022 Urbanizing the floodplain: global changes of imperviousness in flood-prone areas *Environ. Res. Lett.* **17** 104024
Betzold C and Mohamed I 2016 Seawalls as a response to coastal erosion and flooding: a case study from Grande Comore, Comoros (West Indian Ocean) *Reg. Environ. Change* **17** 1077–87
Bonabeau E 2002 Agent-based modeling: methods and techniques for simulating human systems *Proc. Natl Acad. Sci.* **99** 7280–7
Breen M J, Kebede A S and König C S 2022 The safe development paradox in flood risk management: a critical review *Sustainability* **14** 16955
Burby R 2006 Hurricane Katrina and the paradoxes of government disaster policy: bringing about wise governmental decisions for hazardous areas *ANNALS Am. Acad. Political Soc. Sci.* **604** 171–91
Burton C and Cutter S 2008 Levee failures and social vulnerability in the Sacramento-San Joaquin Delta Area, California *Nat. Hazards Rev.* **9** 136–49
Cantwell R 2020 *Estimating the Potential Impact of Climate Change Driven Weather-events on GB Property* (Gamma)
Chandra-Putra H, Zhang H and Andrews C 2015 Modeling real estate market responses to climate change in the coastal zone *J. Artif. Soc. Soc. Simul.* **18** 8
Dawson R, Peppe R and Wang M 2011 An agent-based model for risk-based flood incident management *Nat. Hazards* **59** 167–89
Department for Communities and Local Government 2012 *Technical Guidance to the National Planning Policy Framework* (DCLG)
Di Baldassarre G *et al* 2018 Hess opinions: an interdisciplinary research agenda to explore the unintended consequences of structural flood protection *Hydrol. Earth Syst. Sci.* **22** 5629–37
Di Baldassarre G, Kemerink J, Kooy M and Brandimarte L 2013a Socio-hydrology: conceptualising human-flood interactions *Hydrol. Earth Syst. Sci.* **17** 3295–303
Di Baldassarre G, Kooy M, Kemerink J and Brandimarte L 2013b Towards understanding the dynamic behaviour of floodplains as human-water systems *Hydrol. Earth Syst. Sci.* **17** 3235–44
Di Baldassarre G, Viglione A, Carr G, Kuil L and Yan K 2015 Debates—perspectives on socio-hydrology: capturing feedbacks between physical and social processes *Water Resour. Res.* **51** 4770–81
Du E, Cai X, Sun Z and Minsker B 2017 Exploring the role of social media and individual behaviors in flood evacuation processes: an agent-based modeling approach *Water Resour. Res.* **53** 9164–80
Dubbelboer J, Nikolic I, Jenkins K and Hall J 2017 An agent-based model of flood risk and insurance *J. Artif. Soc. Soc. Simul.* **20** 6
Erdlenbruch K and Bonté B 2018 Simulating the dynamics of individual adaptation to floods *Environ. Sci. Policy* **84** 134–48
Fletcher C 1992 Sea-level trends and physical consequences: applications to the U.S. shore *Earth Sci. Rev.* **33** 73–109
Fusinato E, Han S, Kobiyama M and Madruga de Brito M 2024 Safe development paradox: evidence and methodological insights from a systematic review *Nat. Hazards* **120** 13693–714
Gbadegesin A, Olorunfemi F and Raheem U 2011 Urban vulnerability to climate change and natural hazards in Nigeria *Coping with Global Environmental Change, Disasters and Security* vol 5 pp 669–87
Gotham K, Campanellea R, Lauve-Moon K and Powers B 2018 Hazard experience, geophysical vulnerability, and flood risk perceptions in a postdisaster city, the case of New Orleans *Risk Anal.* **38** 345–56
Haer T, Botzen W and Aerts J 2016 The effectiveness of flood risk communication strategies and the influence of social networks—insights from an agent-based model *Environ. Sci. Policy* **60** 44–52
Haer T, Husby T, Botzen W and Aerts J 2020 The safe development paradox: an agent-based model for flood risk under climate change in the European Union *Glob. Environ. Change* **60** 102009
Han Y, Ash K, Mao L and Peng Z 2020 An agent-based model for community flood adaptation under uncertain sea-level rise *Clim. Change* **162** 2257–76
Janssen M and Ostrom E 2006 Empirically based, agent-based models *Ecol. Soc.* **11** 37
Jongman B, Ward P and Aerts J 2012 Global exposure to river and coastal flooding: long term trends and changes *Glob. Environ. Change* **22** 823–35
Kasmalkar I, Wagenaar D, Bill-Weilandt A, Choong J, Manimaran S, Ning Lim T, Rabonza M and Lallemant D 2023 Flow-tub model: a modified bathtub flood model with hydraulic connectivity and path-based attenuation *MethodsX* **12** 102525
Kates R, Colten C, Laska S, Leatherman P and Clark W 2006 Reconstruction of New Orleans after Hurricane Katrina: a research perspective *Cityscape* **9** 5–22 (available at: www.jstor.org/stable/20868629)
Lee J, Filatova T, Ligmann-Zielinska A, Hassani-Mahmooei B, Stonedahl F, Lorscheid I, Voinov A, Polhill G, Sun Z and Parker D C 2015 The complexities of agent-based modeling output analysis *J. Artif. Soc. Soc. Simul.* **18** 4
Leichenko R 2011 Climate change and urban resilience *Curr. Opin. Environ. Sustain.* **3** 164–8
Loucks D 2015 Debates—perspectives on socio-hydrology: simulating hydrologic-human interactions *Water Resour. Res.* **51** 4789–94
Ludy J and Kondolf G 2012 Flood risk perception in lands "protected" by 100-year levees *Nat. Hazards* **61** 829–42
McNamara D and Keeler D 2013 A coupled physical and economic model of the response of coastal real estate to climate risk *Nat. Clim. Change* **3** 559–62
Metropolitan Borough of Sefton Council 2014 *Sefton Borough Council Local Flood Risk Management Strategy Strategic Environmental Assessment Environmental Report*
Montz B and Tobin G 2008 Livin' large with levees: lessons learned and lost *Nat. Hazards Rev.* **9** 150–7

Müller B et al 2014 Standardised and transparent model descriptions for agent-based models: current status and prospects *Environ. Modelling Softw.* **55** 156–63
Natho S and Thieken A 2018 Implementation and adaptation of a macro-scale method to assess and monitor direct economic losses caused by natural hazards *Int. J. Disaster Risk Reduct.* **28** 191–205
Ridolfi E, Mondino E and Di Baldassarre G 2021 Hydrological risk: modeling flood memory and human proximity to rivers *Hydrol. Res.* **51** 241–52
Sanders B and Grant S 2020 Re-envisioning stormwater infrastructure for ultrahazardous flooding *WIREs Water* **7** 1414
Schoppa L, Barendrecht M, Paprotny D, Sairam N, Sieg T and Kreibich H 2024 Projecting flood risk dynamics for effective long-term adaptation *Earth's Future* **12** 022EF003258
Sharples J, Cary G, Fox-Hughes P, Mooney S, Evans J, Fletcher M, Fromm M, Grierson P, McRae R and Baker P 2016 Natural hazards in Australia: extreme bushfire *Clim. Change* **139** 85–99
Smajgl A, Brown D G, Valbuena D and Huigen M G A 2011 Empirical characterisation of agent behaviours in socio-ecological systems *Environ. Modelling Softw.* **26** 837–44
Sobiech C 2013 *Agent-Based Simulation of Vulnerability Dynamics: A Case Study of the German North Sea Coast* (Springer)
Sun Z et al 2016 Simple or complicated agent-based models? A complicated issue *Environ. Modelling Softw.* **86** 56–67
Tellman B, Sullivan J, Kuhn C, Kettner A, Doyle C, Brakenridge G, Erickson T and Slayback D 2021 Satellite imaging reveals increased proportion of population exposed to floods *Nature* **596** 80–86
Tesselaar M, Botzen W, Tiggeloven T and Aerts J 2023 Flood insurance is a driver of population growth in European floodplains *Nat. Commun.* **14** 7483
Tobin G 1995 The levee love affair: a stormy relationship? *J. Am. Water Res. Assoc.* **31** 359–67
Troy T, Konar M, Srinivasan V and Thompson S 2015 Moving sociohydrology forward: a synthesis across studies *Hydrol. Earth Syst. Sci.* **19** 3667–79
Vora A, Sharma P, Loliyana V, Patel P and Timbadiya P 2018 Assessment and prioritization of flood protection levees along the lower Tapi River, India *Nat. Hazards Rev.* **19** 05018009
White G 1945 *Human Adjustment to Floods* (University of Chicago)